NATIONAL ADVISORY COMMITTEE FOR AERONAUTICS

WARTIME REPORT

ORIGINALLY ISSUED

April 1945 as
Advance Restricted Report L5C13

INVESTIGATION OF EFFECT OF SIDESLIP ON LATERAL STABILITY CHARACTERISTICS II - RECTANGULAR MIDWING ON CIRCULAR FUSELAGE WITH VARIATIONS IN VERTICAL-TAIL AREA AND FUSELAGE LENGTH WITH AND WITHOUT HORIZONTAL TAIL SURFACE

By Thomas A. Hollingworth

Langley Memorial Aeronautical Laboratory
Langley Field, Va.

WASHINGTON

NATIONAL ADVISORY COMMITTEE FOR AERONAUTICS

ADVANCE RESTRICTED REPORT

INVESTIGATION OF EFFECT OF SIDESLIP ON LATERAL STABILITY CHARACTERISTICS II - RECTANGULAR MIDWING ON CIRCULAR FUSELAGE WITH VARIATIONS IN VERTICAL-TAIL AREA AND FUSELAGE LENGTH WITH AND WITHOUT HORIZONTAL TAIL SURFACE

By Thomas A. Hollingworth

SUMMARY

Power-off tests were made in the 6- by 6-foot test section of the Langley stability tunnel to determine the variation of the static lateral stability characteristics with vertical-tail area, fuselage length, and wing dihedral. Two NACA 23012 rectangular wings with rounded tips and dihedral angles of 0° and 5° were tested alone and in combination with three circular fuselages of different lengths. The wing-fuselage combinations were tested as midwing monoplanes with and without a horizontal tail and with variations in vertical-tail area. The results are presented as curves showing the variation of the static-lateral-stability slopes with angle of attack, and the rolling-moment, yawing-moment, and lateral-force coefficients with angle of yaw.

The results indicated that the wing-fuselage interference on the slope of the curve of yawing-moment coefficient against angle of yaw C_{n_ψ} and on the slope of the curve of lateral-force coefficient against angle of yaw C_{Y_ψ} was small and remained practically constant over the unstalled angle-of-attack range. In the high-speed flight range, the wing-fuselage interference on the vertical tail was small and, in the normal flight range, was not appreciably changed by an increase in fuselage length or vertical-tail area for the sizes investigated.

With no vertical tail, increased fuselage length caused a negligible change in C_{n_ψ} for the fuselage lengths tested. For the complete model, C_{n_ψ} increased approximately linearly with fuselage length. The slopes C_{n_ψ} and C_{Y_ψ} increased approximately linearly with vertical-tail area. For the system of axes used, the slope of the curve of rolling-moment coefficient against angle of yaw C_{l_ψ} increased with vertical-tail area at negative and small positive angles of attack but decreased at large positive angles of attack. The results also indicated that increased dihedral angle slightly decreased the rate of change of C_{n_ψ} with vertical-tail area but had a negligible effect on the rate of change of C_{n_ψ} with fuselage length. An appreciable increase in C_{n_ψ} was caused by the end-plate effect of the horizontal tail on the vertical tail.

INTRODUCTION

The trend toward greater speed and higher wing loadings and the increased consciousness of the importance of satisfactory flying qualities have resulted in additional attention being given to handling characteristics in airplane design. Mathematical equations and convenient charts for predicting the lateral stability characteristics are given in reference 1. In order to use this material, however, it is necessary to know the stability derivatives, which vary with each airplane configuration. A series of investigations has therefore been undertaken in the Langley stability tunnel to determine the variation of both the static-stability and rotary-stability slopes with various airplane parameters.

The present investigation is a continuation of the investigation described in reference 2 except that, for the present tests, the fuselage was equipped with a rectangular wing in the midposition. The purpose of the investigation, which was conducted in the 6- by 6-foot test section of the Langley stability tunnel, was to determine experimentally the effect, with the propeller off, of vertical-tail area, fuselage length, wing dihedral, interference, and the presence of the horizontal tail on

the static lateral stability characteristics. A geometrically similar model has been tested in the Langley 7- by 10-foot tunnel (reference 3) and the data may be used to correlate the results in the two tunnels.

Tests were made of a model that had dimensions proportional to those of the average airplane. The ratios of fuselage length to wing span and of vertical-tail area to wing area investigated were taken to bracket the range commonly used on present-day airplanes.

APPARATUS AND MODEL

The tests were made in the 6- by 6-foot closed-throat test section (adjusted for straight flow) of the Langley stability tunnel.

A three-view drawing of the model tested, which was constructed of laminated mahogany, is given in figure 1. Figure 2 shows the model mounted on the three support struts for tests in the tunnel.

The two rectangular wings used for the tests have dihedral angles of 0° and 5° and, in elevation, the maximum upper-surface section ordinates are in one plane. Each has an aspect ratio of 6.4 and an area of 361 square inches, which includes the portion inside the fuselage. The NACA 23012 profile is maintained along the entire span.

The fuselage is of circular cross section and was constructed as described in reference 2. Its dimensions are presented in table I. With the shortest tail cone attached, the fuselage is geometrically similar to that of reference 3.

Five interchangeable vertical tails and the horizontal tail were made to the NACA 0009 section (fig. 1). Their dimensions are presented in table II.

TESTS

The wings with dihedral angles of 0° and 5° were tested alone at angles of yaw of -5° and 5° over an

angle-of-attack range from -10° to 20°. The model combinations tested are shown in table III. Model combinations were tested at angles of yaw of -5°, 0°, and 5° over an angle-of-attack range from -10° to 20° and at angles of attack of -0.2° and 10.3° over an angle-of-yaw range from -30° to 12°.

Tests in which the angle of attack was varied were run at a dynamic pressure of 65 pounds per square foot, which corresponds to a Reynolds number of approximately 888,000 based on an 8-inch wing chord. Tests in which the angle of yaw was varied were run at a dynamic pressure of 65 pounds per square foot at an angle of attack of -0.2° and at 40 pounds per square foot, which corresponds to a Reynolds number of about 546,000, at an angle of attack of 10.3° to minimize the possibility of compressibility effects at large angles of attack.

The rolling-moment data are not presented for a few tests, because the tare readings were inconsistent.

PRESENTATION OF DATA

The results of the tests are presented in standard NACA coefficients of forces and moments. Rolling-moment and yawing-moment coefficients are given about the center-of-gravity location shown in figure 1. The data are referred to the stability axes, which are a system of axes having their origin at the center of gravity and in which the Z-axis is in the plane of symmetry and perpendicular to the relative wind, the X-axis is in the plane of symmetry and perpendicular to the Z-axis, and the Y-axis is perpendicular to the plane of symmetry.

The coefficients and symbols used are defined as follows:

C_L lift coefficient $\left(L/qS_w\right)$

C_D drag coefficient $\left(D/qS_w\right)$

C_Y lateral-force coefficient $\left(Y/qS_w\right)$

C_{Y_ψ} slope of curve of lateral-force coefficient against angle of yaw $\left(\partial C_Y/\partial\psi\right)$

C_l rolling-moment coefficient $\left(L'/qbS_w\right)$

C_{l_ψ} slope of curve of rolling-moment coefficient against angle of yaw $\left(\partial C_l/\partial \psi\right)$

C_n yawing-moment coefficient $\left(N/qbS_w\right)$

C_{n_ψ} slope of curve of yawing-moment coefficient against angle of yaw $\left(\partial C_n/\partial \psi\right)$

Δ_1 increment of C_{n_ψ} or C_{Y_ψ} caused by wing-fuselage interference

Δ_2 increment of C_{n_ψ} or C_{Y_ψ} caused by wing-fuselage interference on vertical tail

$\frac{lS_v}{bS_w}$ tail-volume coefficient

D force along X-axis; positive when directed downstream

Y force along Y-axis; positive when directed to the right

L force along Z-axis; positive when directed upward

N yawing moment about Z-axis; positive when tends to retard right wing

L' rolling moment about X-axis; positive when tends to depress right wing

q dynamic pressure $\left(\frac{1}{2}\rho V^2\right)$

V free-stream velocity

ρ mass density of air

S_w wing area (2.507 sq ft)

b wing span (4 ft)

Γ dihedral angle, degrees

l tail length; measured from center of gravity, which is assumed to be 10.40 inches behind nose of model on center line of fuselage, to hinge line of tail surface

S_v vertical-tail area

α angle of attack, degrees

ψ angle of yaw, degrees

The static-lateral-stability slopes C_{n_ψ}, C_{l_ψ}, and C_{Y_ψ} were obtained from data measured at $\psi = \pm 5^\circ$ since the yaw tests showed that the coefficients had an approximately linear variation in the range of angle of yaw from 5° to -5°. In order to indicate the validity of this procedure, the slopes obtained from yaw tests at $\psi = 0^\circ$ are plotted with tailed symbols in the figures.

The accuracy of C_n, C_l, and C_Y was determined experimentally to be about ± 0.0005, ± 0.0008, and ± 0.001, respectively, at a dynamic pressure of 65 pounds per square foot. The average experimental accuracy of C_{n_ψ}, C_{l_ψ}, and C_{Y_ψ} is about ± 0.00010, ± 0.00016, and ± 0.0002, respectively. The accuracies of the angle-of-attack and angle-of-yaw measurements are about 0.1° and 0.05°, respectively.

Angle of attack and drag coefficient were corrected for tunnel-wall effect by the following formulas:

$$\Delta\alpha = 57.3\delta_w \frac{S_w}{C} C_L = 0.609 C_L \quad \text{(deg)}$$

$$\Delta C_D = \delta_w \frac{S_w}{C} C_L^2 = 0.0106 C_L^2$$

where

δ_w jet-boundary correction factor at wing (0.1525)

C cross-sectional area of tunnel (36 sq ft)

Both corrections are additive. No jet-boundary corrections were applied to C_l, C_n, and C_Y. The correction to C_Y is within the experimental error, whereas the corrections to C_n and C_l would be subtractive and equal to about 1 percent.

The C_L and C_D data were corrected for the support-strut effect; no corrections were applied to C_Y, C_l, or C_n since previous results indicated the magnitude of these corrections to be small for this model and support system.

The values of Δ_1 and Δ_2 for C_{n_ψ} for the model without wing fillets were obtained by the following formulas:

$$\Delta_1 C_{n_\psi} = C_{n_\psi}{}_{\text{wing-fuselage combination}} - \left(C_{n_\psi}{}_{\text{wing}} + C_{n_\psi}{}_{\text{fuselage}}\right)$$

$$\Delta_2 C_{n_\psi} = C_{n_\psi}{}_{\text{complete model}} - \left(C_{n_\psi}{}_{\text{wing}} + C_{n_\psi}{}_{\text{fuselage with hor. and vert. tails on}} + \Delta_1 C_{n_\psi}\right)$$

The values of Δ_1 and Δ_2 for C_{Y_ψ} may be obtained in the same manner. The method used to obtain Δ_1 and Δ_2 is the same as that of reference 4. The following formula (by which the value of C_{n_ψ} for the complete model is obtained) is an example of the application of the increments Δ_1 and Δ_2:

$$C_{n_\psi} = C_{n_\psi}{}_{\text{wing}} + C_{n_\psi}{}_{\text{fuselage with hor. and vert. tails on}} + \Delta_1 C_{n_\psi} + \Delta_2 C_{n_\psi}$$

The interference between the fuselage and vertical tail and the interference between the fuselage and horizontal tail were not determined.

Lift-coefficient and drag-coefficient data for representative model configurations are shown in figure 3. The lateral-stability slopes C_{n_ψ} and C_{Y_ψ} for the wing

are presented in figure 4. The data presented in the figures are summarized in table IV.

DISCUSSION

The static-lateral-stability slopes C_{n_ψ} and C_{Y_ψ} remained practically constant over the unstalled angle-of-attack range (figs. 9 to 13, 15, and 16). With the system of axes used, the center of pressure of the vertical tail varied with respect to the X-axis. At negative and small positive angles of attack, the center of pressure was above the X-axis and, therefore, the side force on the vertical tail caused a positive increment of C_{l_ψ}. The opposite was true at large positive angles of attack, since the center of pressure of the vertical tail was below the X-axis.

The jags in the curves of lateral-force, rolling-moment, and yawing-moment coefficients noted in figures 8, 13, 16, and 18 can probably be attributed to vertical-tail stalling.

Interference Effects

The increments caused by wing-fuselage interference Δ_1 and by wing-fuselage interference on the vertical tail Δ_2 were computed by the equations previously given. The fuselage data (with and without tail surfaces) used in these computations were taken from reference 2. The other data were obtained from the present investigation.

The magnitudes of $\Delta_1 C_{n_\psi}$ and $\Delta_1 C_{Y_\psi}$ are small and remained practically constant over the unstalled angle-of-attack range (fig. 5). The change in the magnitude of these quantities with fuselage length was within the experimental accuracy for the fuselage lengths tested.

Both $\Delta_2 C_{n_\psi}$ and $\Delta_2 C_{Y_\psi}$ varied appreciably with angle of attack but their magnitudes were small in the high-speed flight range. (See fig. 6.) Replacing vertical tail 2 by vertical tail 4 (a 48-percent

increase in area) only slightly changed the magnitude of these quantities in the normal flight range. As indicated by previous experimental data (reference 4), the variation of $\Delta_2 C_{n_\psi}$ and $\Delta_2 C_{Y_\psi}$ with the fuselage lengths tested was generally small in the normal flight range.

Effect of Horizontal Tail

Theory indicates that the presence of the horizontal tail increases the effective aspect ratio of the vertical tail and thus increases C_{n_ψ} and C_{Y_ψ} (reference 5). A pronounced increase in these quantities was obtained in the present investigation by the addition of the horizontal tail. This increase diminished somewhat with a positive increase in angle of attack. (See figs. 7 and 8.) A correlation of the results of previous airfoil tests in the Langley stability tunnel indicates a value of 0.105 for the section lift-curve slope of an NACA 0009 airfoil. By substituting this value for the theoretical section lift-curve slope of 0.109 in equation (4) of reference 6 and by the use of figure 5 in reference 5, an incremental increase in C_{Y_ψ} of 0.0010 was computed for the end-plate effect of the horizontal tail on vertical tail 4. An average experimental increment of 0.0010 was obtained for the model with a dihedral angle of 0° and 0.0015 for the model with a dihedral angle of 5°. The end-plate effect of the horizontal tail on C_{l_ψ} amounted to about 1° of effective dihedral.

With the vertical tail off, the magnitude of the static-lateral-stability slopes was not appreciably affected by the addition of the horizontal tail. (See figs. 9 and 11.)

Effect of Changes in Fuselage Length

Within the scope of the present investigation, a negligible increase in C_{n_ψ} was obtained by increasing the fuselage length for the model with no vertical tail. (See figs. 9 to 11.) For the complete model equipped with vertical tail 4, the increase in C_{n_ψ} with fuselage

length was approximately linear and fairly constant over the unstalled angle-of-attack range. (See figs. 12 to 14.) The variation in C_{l_ψ} and C_{Y_ψ} was small both with and without a vertical tail for the fuselage lengths tested.

Effect of Changes in Vertical-Tail Area

The increases in C_{n_ψ} and C_{Y_ψ} with vertical-tail area were approximately linear and the magnitudes were nearly constant over the unstalled angle-of-attack range. (See figs. 14 to 16.) As would be expected, at negative and small positive angles of attack, C_{l_ψ} increased with vertical-tail area whereas, at large positive angles of attack, C_{l_ψ} decreased with increased vertical-tail area.

Effect of Changes with Constant Tail Volume

In figures 17 and 18 the result of changing the fuselage length and vertical-tail area in such a manner as to hold the tail volume constant is shown. The configurations tested in which the tail volume remained constant are shown in table V. Data from figures 17 and 18 are cross-plotted in figure 14. All the vertical tails tested had an aspect ratio of 2.15.

The slope C_{n_ψ} should remain approximately the same with constant tail volume. The small experimental variation is possibly caused by interference or might be explained by the arbitrary manner in which the tail-volume coefficient was defined.

The values of C_{l_ψ} and C_{Y_ψ} are dependent mainly on vertical-tail area and are practically independent of tail length (fig. 14). For the range of variations giving constant tail volume, the change in C_{l_ψ} was not more than about 0.0002, which is equivalent to about 1° of effective dihedral.

Effect of Changes in Dihedral

The slope C_{Y_ψ} generally was slightly greater for $\Gamma = 5^\circ$ than for $\Gamma = 0^\circ$. (See figs. 9 to 13, 15, and 16.) With the vertical tail off, the change in C_{n_ψ} with dihedral angle was insignificant (figs. 9 to 11) but, with the vertical tail on, C_{n_ψ} was slightly larger for $\Gamma = 0^\circ$ than for $\Gamma = 5^\circ$ (figs. 12 to 16). Figure 14 shows that increased dihedral angle slightly decreased the rate of change of C_{n_ψ} with vertical-tail area but had a negligible effect on the rate of change of C_{n_ψ} with fuselage length.

The change with dihedral angle of wing-fuselage interference and wing-fuselage interference on the vertical tail was small.

Comparison of Data from Langley 7- by 10-Foot and Langley Stability Tunnels

The model tested in the Langley stability tunnel is 0.8 as large and geometrically similar to the one tested in the Langley 7- by 10-foot tunnel for the investigation of reference 3. The test Reynolds number, based on the wing chord, was about 619,000 for the Langley 7- by 10-foot tunnel compared with about 888,000 for the Langley stability tunnel. The effective Reynolds number, however, was about the same since the turbulence factor for the Langley 7- by 10-foot tunnel is 1.6 compared with less than 1.1 for the Langley stability tunnel. Data taken from reference 3 were converted to the stability axes and the angle of attack was corrected for tunnel-wall effect in order to make the data comparable with data from the Langley stability tunnel. Figure 19 shows that satisfactory agreement was obtained for all three static-lateral-stability slopes. In both tunnels the model, when yawed, tended to roll violently at the stall.

CONCLUSIONS

The results of tests of a model consisting of a rectangular midwing on a circular fuselage with variations

in vertical-tail area and fuselage length with and without a horizontal tail indicated, for the range of configurations tested, the following conclusions:

1. The wing-fuselage interference on the slope of the curve of yawing-moment coefficient against angle of yaw C_{n_ψ} and the slope of the curve of lateral-force coefficient against angle of yaw C_{Y_ψ} was small and remained practically constant over the unstalled angle-of-attack range. In the high-speed flight range, the wing-fuselage interference on the vertical tail was small and, in the normal flight range, was not appreciably changed by fuselage length or by an increase of about 48 percent in vertical-tail area.

2. The end-plate effect of the horizontal tail on the vertical tail appreciably increased C_{n_ψ} and C_{Y_ψ}. Good agreement was obtained between experimental and computed values of C_{Y_ψ}.

3. Increasing the fuselage length with no vertical tail resulted in a negligible change in C_{n_ψ} for the model, both with and without a horizontal tail. For the complete model, the increase in C_{n_ψ} was approximately linear with fuselage length. The changes in the slope of the curve of rolling-moment coefficient against angle of yaw C_{l_ψ} and in C_{Y_ψ} with fuselage length were small.

4. The increases in C_{n_ψ} and C_{Y_ψ} with vertical-tail area were approximately linear. For the system of axes used, an increase in vertical-tail area increased C_{l_ψ} at negative and small positive angles of attack but the opposite was true at large positive angles of attack.

5. Increased dihedral angle slightly decreased the rate of change of C_{n_ψ} with vertical-tail area but had a negligible effect on the rate of change of C_{n_ψ} with fuselage length.

Langley Memorial Aeronautical Laboratory
National Advisory Committee for Aeronautics
Langley Field, Va.

REFERENCES

1. Zimmerman, Charles H.: An Analysis of Lateral Stability in Power-Off Flight with Charts for Use in Design. NACA Rep. No. 589, 1937.

2. Fehlner, Leo F., and MacLachlan, Robert: Investigation of Effect of Sideslip on Lateral Stability Characteristics. I - Circular Fuselage with Variations in Vertical-Tail Area and Tail Length with and without Horizontal Tail Surface. NACA ARR No. L4E25, 1944.

3. Bamber, M. J., and House, R. O.: Wind-Tunnel Investigation of Effect of Yaw on Lateral-Stability Characteristics. II - Rectangular N.A.C.A. 23012 Wing with a Circular Fuselage and a Fin. NACA TN No. 730, 1939.

4. Recant, Isidore G., and Wallace, Arthur R.: Wind-Tunnel Investigation of Effect of Yaw on Lateral-Stability Characteristics. III - Symmetrically Tapered Wing at Various Positions on Circular Fuselage with and without a Vertical Tail. NACA TN No. 825, 1941.

5. Katzoff, S., and Mutterperl, William: The End-Plate Effect of a Horizontal-Tail Surface on a Vertical-Tail Surface. NACA TN No. 797, 1941.

6. Jones, Robert T.: Theoretical Correction for the Lift of Elliptic Wings. Jour. Aero. Sci., vol. 9, no. 1, Nov. 1941, pp. 8-10.

TABLE I

FUSELAGE DIMENSIONS

Fuselage	Fuselage length (in.)	Tail-cone length (in.)	Tail length, l (in.)	$\frac{\text{Tail length}}{\text{Wing span}}, \frac{l}{b}$
Short	32.25	9.85	20.07	0.418
Medium	37.05	14.65	24.87	.518
Long	41.85	19.45	29.67	.618

TABLE II

TAIL-SURFACE DIMENSIONS

Tail surface	Designation	Tail area (sq in.) (1)	$\frac{\text{Tail area}}{\text{Wing area}}$	Aspect ratio
Vertical	1	10.83	0.0300	2.15
Do---	2	23.78	.0659	2.15
Do---	3	28.37	.0786	2.15
Do---	4	35.16	.0974	2.15
Do---	5	46.20	.1280	2.15
Horizontal	----------	64.21	.178	3.99

[1]Area measured from root chord at center line of fuselage.

TABLE III

MODEL COMBINATIONS TESTED

[$\Gamma = 0^\circ$ and 5°]

Horizontal tail	Vertical tail	Fuselage	Variable
On	Off	Short, medium, and long	α
	1		
	2		
	3		
	4		
	5		
	2	Long	ψ
	4		
	3	Medium	
	4		
	4	Short	
Off	Off	Short	α and ψ
	Off	Long	
	4	Short	

TABLE IV

PRESENTATION OF RESULTS

Figure	Description of figure	Data presented
3	Lift and drag curves for representative model configuration	C_L and C_D as f(α)
4	Slope of yawing-moment and lateral-force coefficients for NACA 23012 rectangular wing	C_{n_ψ} and C_{Y_ψ} as f(α)
5	Effect of wing-fuselage interference	$\Delta_1 C_{n_\psi}$ and $\Delta_1 C_{Y_\psi}$ as f(α)
6	Effect of wing-fuselage interference on vertical tail	$\Delta_2 C_{n_\psi}$ and $\Delta_2 C_{Y_\psi}$ as f(α)
7	End-plate effect of horizontal tail	C_{n_ψ}, C_{l_ψ}, and C_{Y_ψ} as f(α)
8	End-plate effect of horizontal tail	C_n, C_l, and C_Y as f(ψ)
9	Effect of changing fuselage length (no tail surfaces)	C_{n_ψ}, C_{l_ψ}, and C_{Y_ψ} as f(α)
10	Effect of changing fuselage length (no tail surfaces)	C_n, C_l, and C_Y as f(ψ)
11	Effect of changing fuselage length (horizontal tail on; vertical tail off)	C_{n_ψ}, C_{l_ψ} and C_{Y_ψ} as f(α)
12	Effect of changing fuselage length (horizontal tail and vertical tail 4 on)	C_{n_ψ}, C_{l_ψ}, and C_{Y_ψ} as f(α)
13	Effect of changing fuselage length (horizontal tail and vertical tail 4 on)	C_n, C_l, and C_Y as f(ψ)

TABLE IV - Concluded

PRESENTATION OF RESULTS - Concluded

Figure	Description of figure	Data presented
14	Effect of changing fuselage length	C_{n_ψ}, C_{l_ψ}, and C_{Y_ψ} as f $\left(\frac{S_V}{S_W}\right)$
15	Effect of changing vertical-tail area	C_{n_ψ}, C_{l_ψ}, and C_{Y_ψ} as f(α)
16	Effect of changing vertical-tail area	C_n, C_l, and C_Y as f(ψ)
17	Effect of changes with tail volume constant	C_{n_ψ}, C_{l_ψ}, and C_{Y_ψ} as f(α)
18	Effect of changes with tail volume constant	C_n, C_l, and C_Y as f(ψ)
19	Comparison of data from Langley stability and Langley 7- by 10-foot tunnels	C_{n_ψ}, C_{l_ψ}, and C_{Y_ψ} as f(α)

NATIONAL ADVISORY
COMMITTEE FOR AERONAUTICS

TABLE V

MODEL CONFIGURATIONS HAVING CONSTANT TAIL VOLUME

Vertical tail	Fuselage	$\frac{\text{Tail length}}{\text{Wing span}}, \frac{l}{b}$	$\frac{\text{Tail area}}{\text{Wing area}}, \frac{S_v}{S_w}$	Tail-volume coefficient, $\frac{lS_v}{bS_w}$
4	Short	0.418	0.0974	0.0407
3	Medium	.518	.0786	.0407
2	Long	.618	.0659	.0407

NATIONAL ADVISORY
COMMITTEE FOR AERONAUTICS

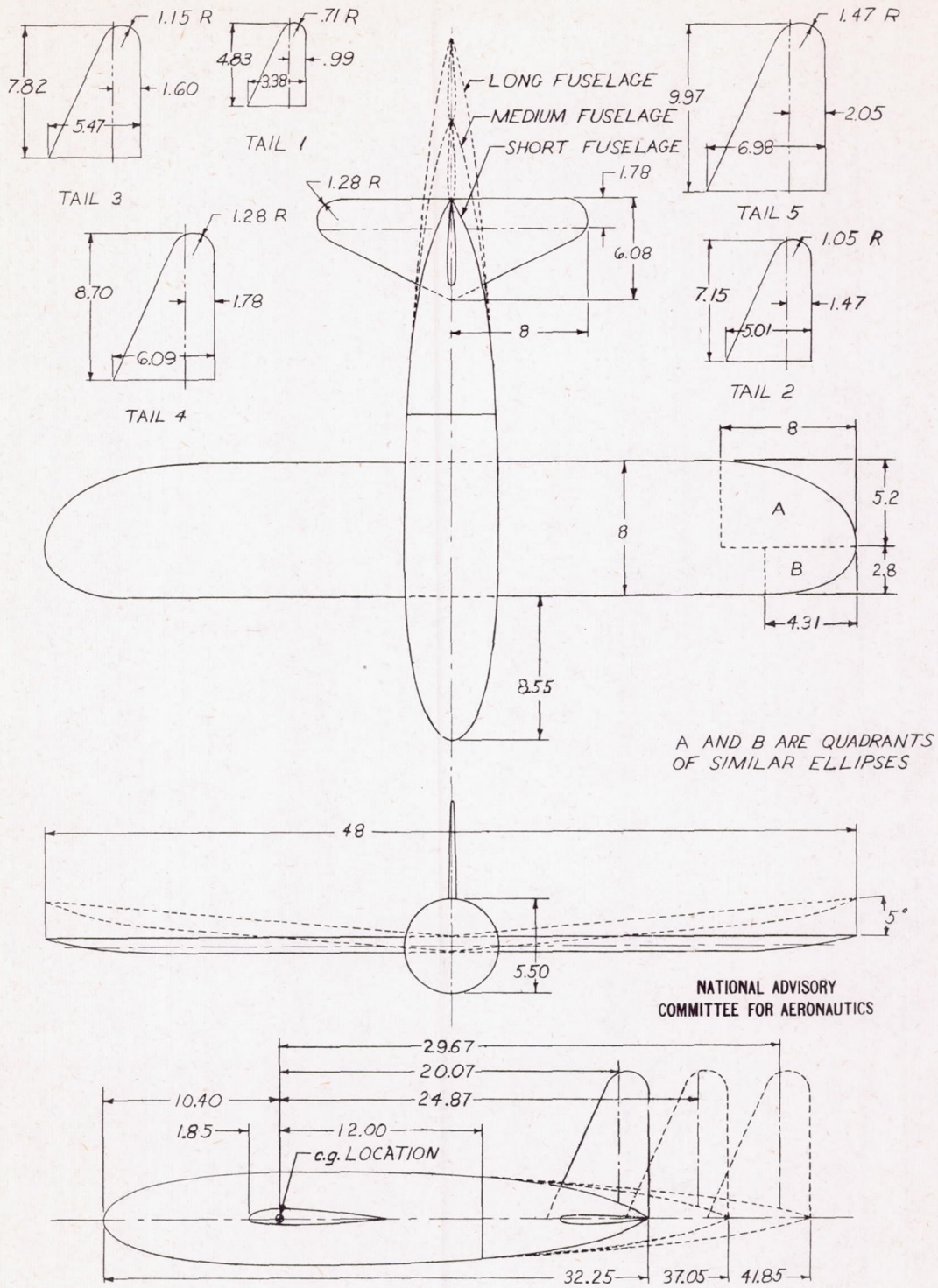

Figure 1.- Rectangular NACA 23012 wing in combination with circular fuselage, vertical and horizontal tails, and tail cones. All dimensions given in inches.

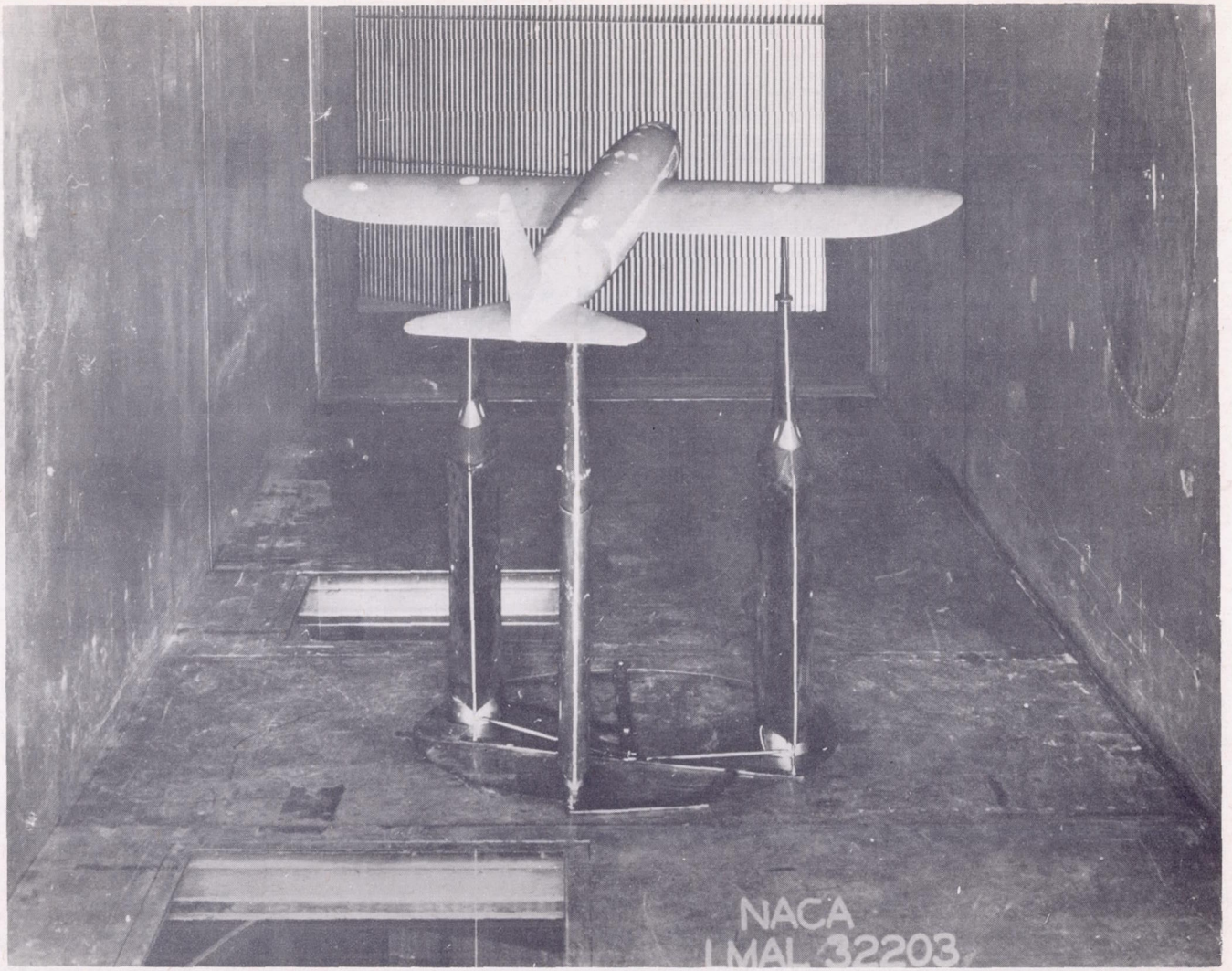

Figure 2.- Rectangular-midwing model equipped with short fuselage and vertical tail 5 mounted for tests in Langley stability tunnel.

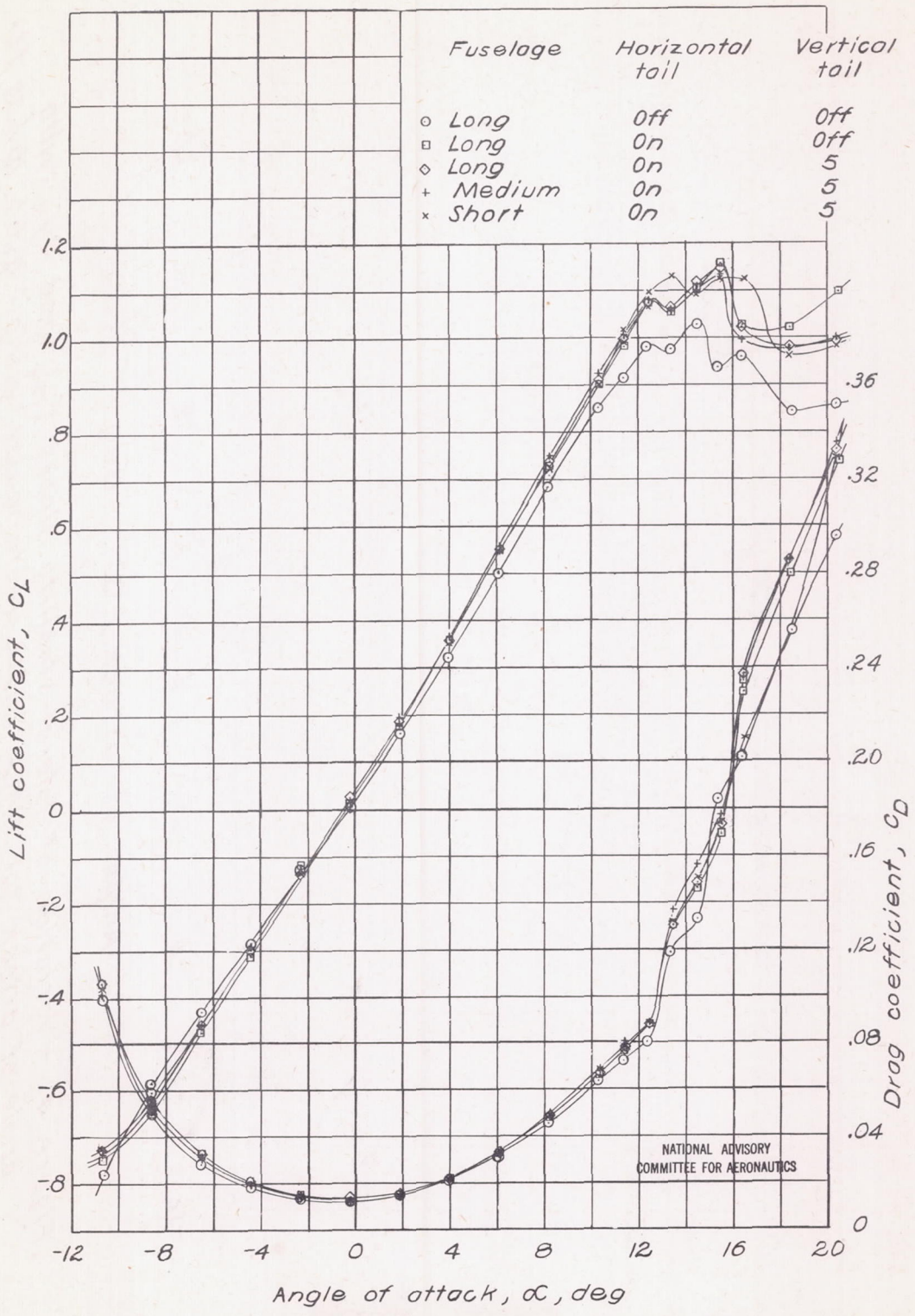

Figure 3.- Variation of lift and drag coefficients with angle of attack for representative model configurations. Γ, 5°; ν, 0°; q, 65 lb/sq ft.

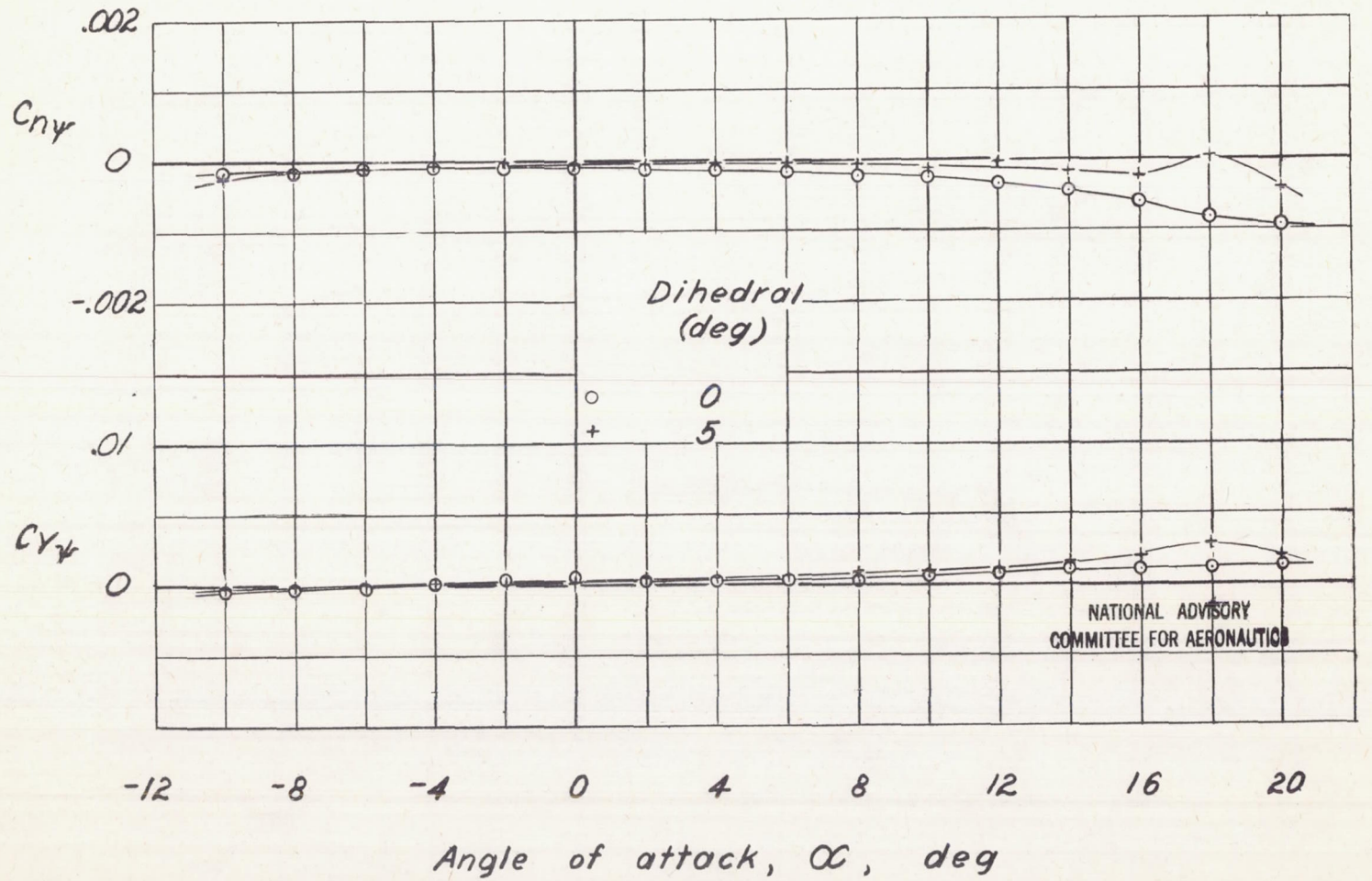

Figure 4.- Variation of lateral-stability slopes C_{n_ψ} and C_{Y_ψ} with angle of attack for NACA 23012 rectangular wing. q, 65 lb/sq ft.

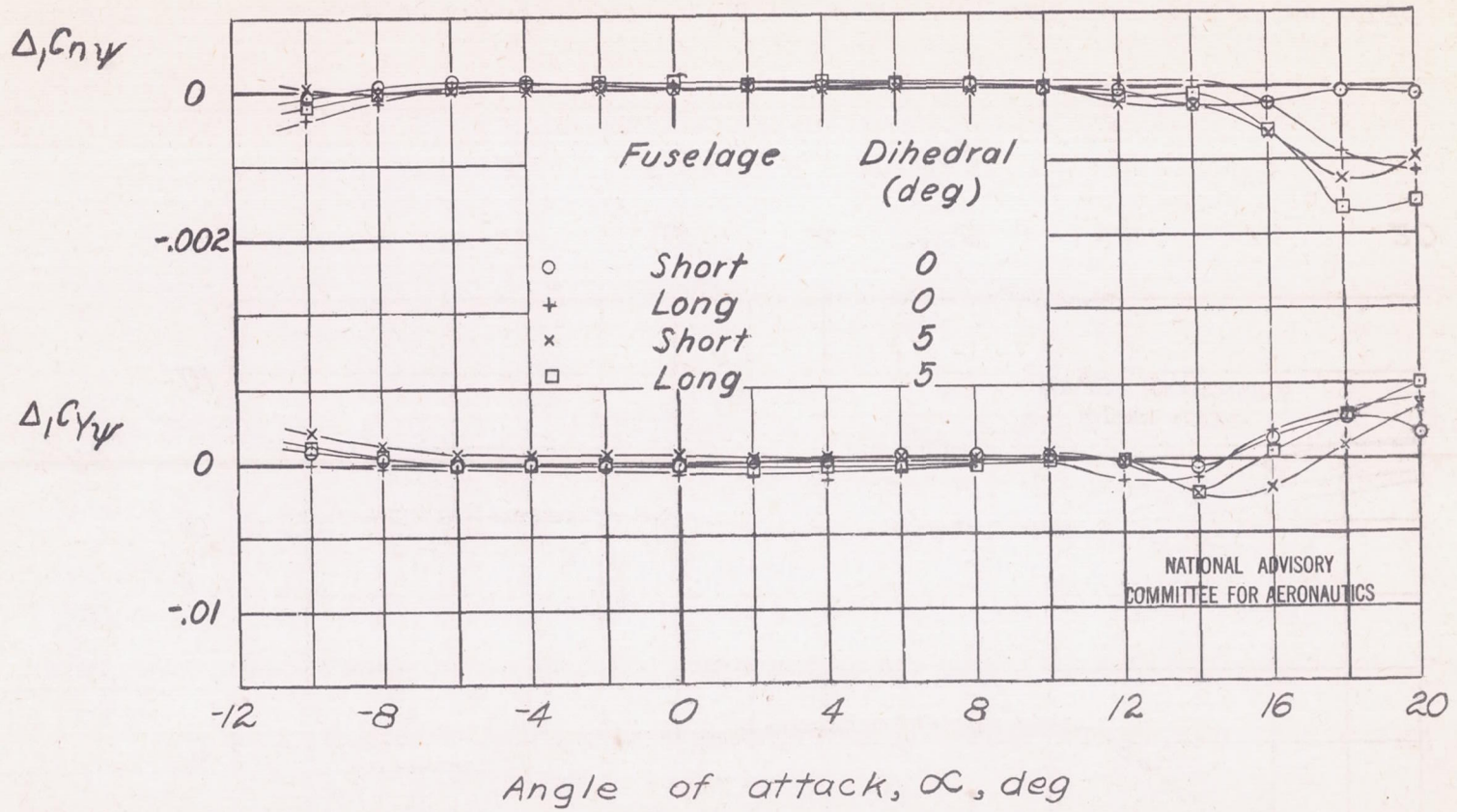

Figure 5.- Increments of C_{n_ψ} and C_{Y_ψ} due to wing-fuselage interference. Horizontal and vertical tails off; q, 65 lb/sq ft.

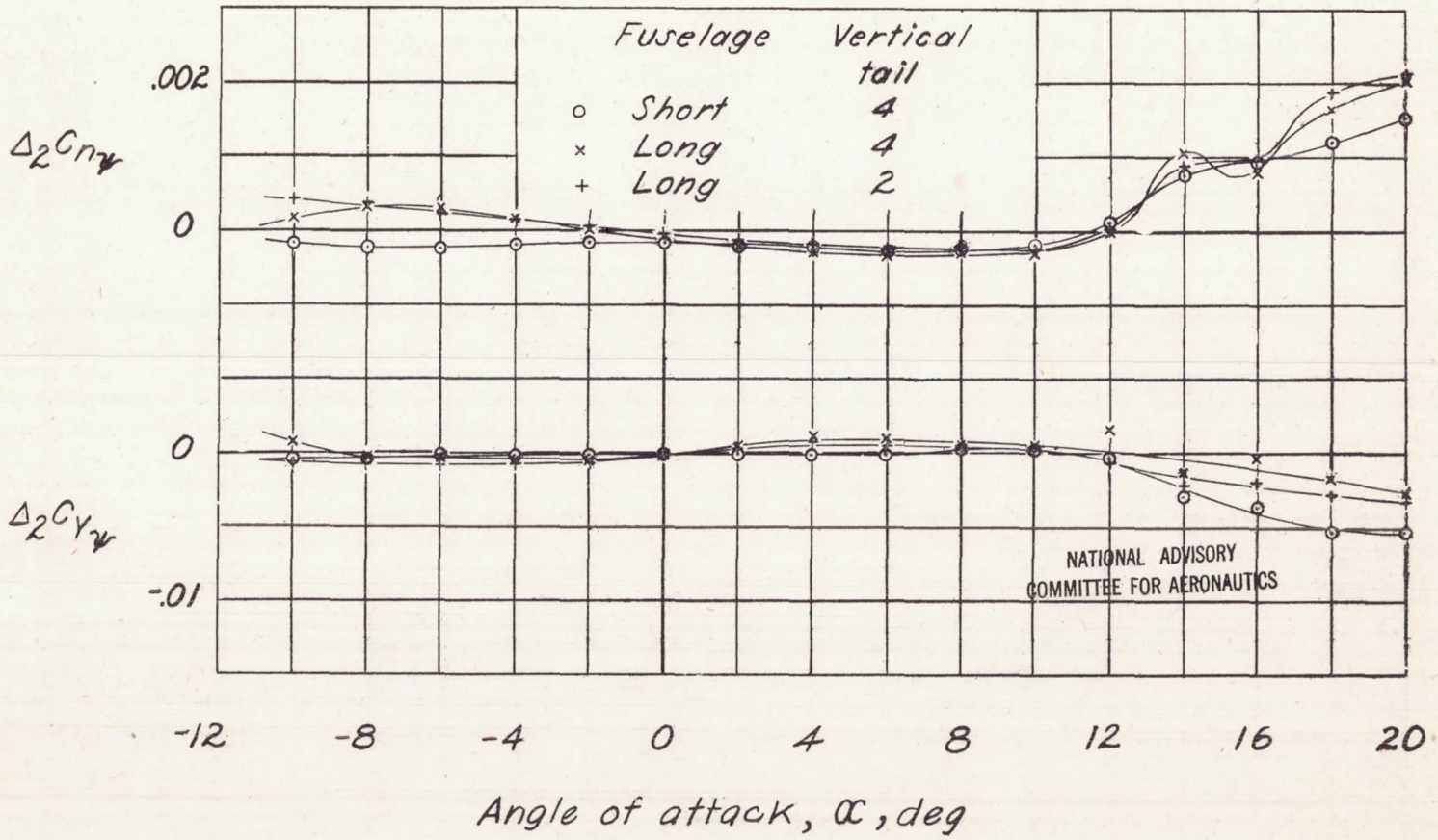

(a) Γ, 0°.

Figure 6.- Increments of Cn_ψ and Cy_ψ due to wing-fuselage interference on vertical tail. Horizontal tail on; q, 65 lb/sq ft.

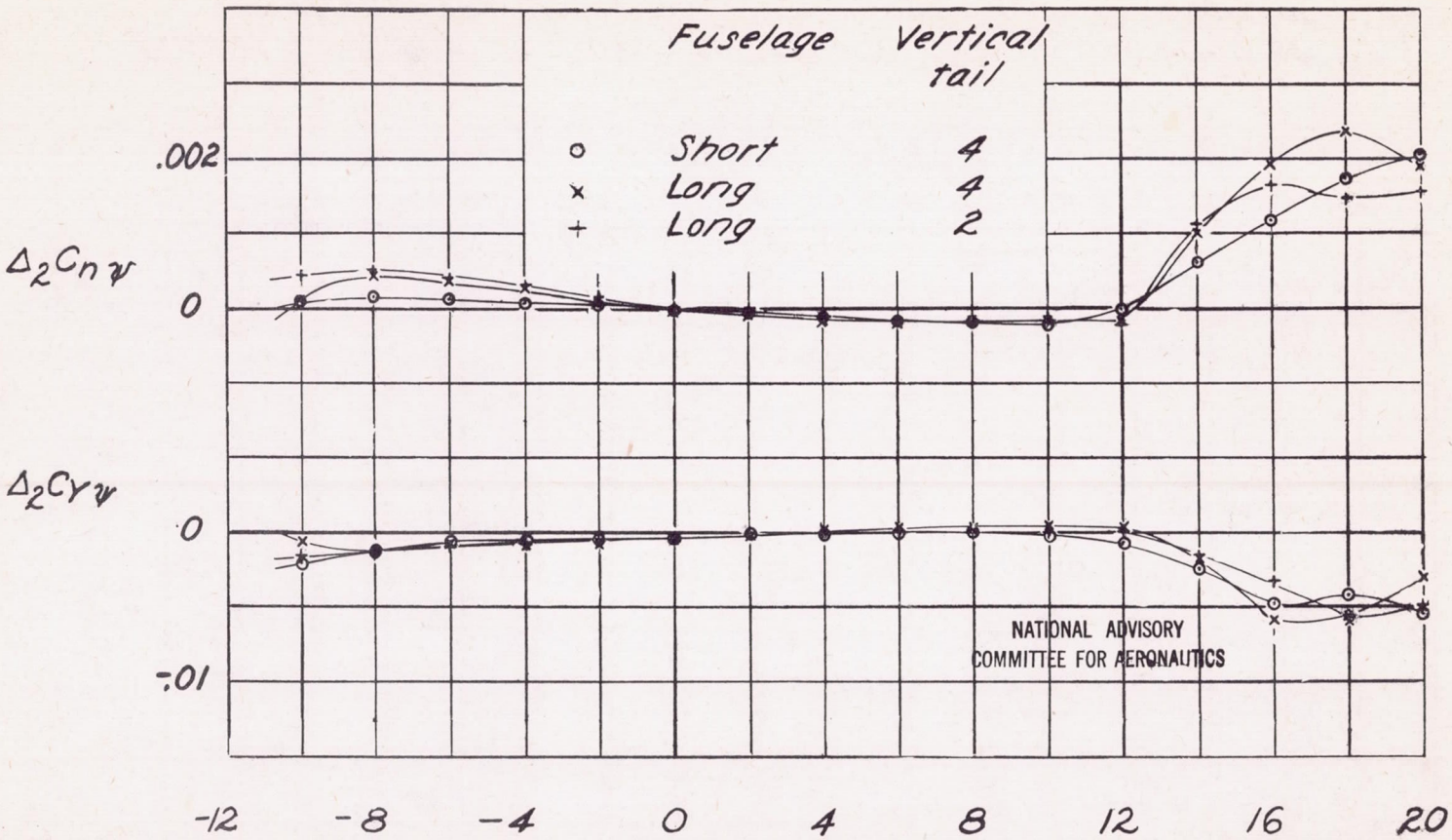

(b) Γ, 5°.

Figure 6.- Concluded.

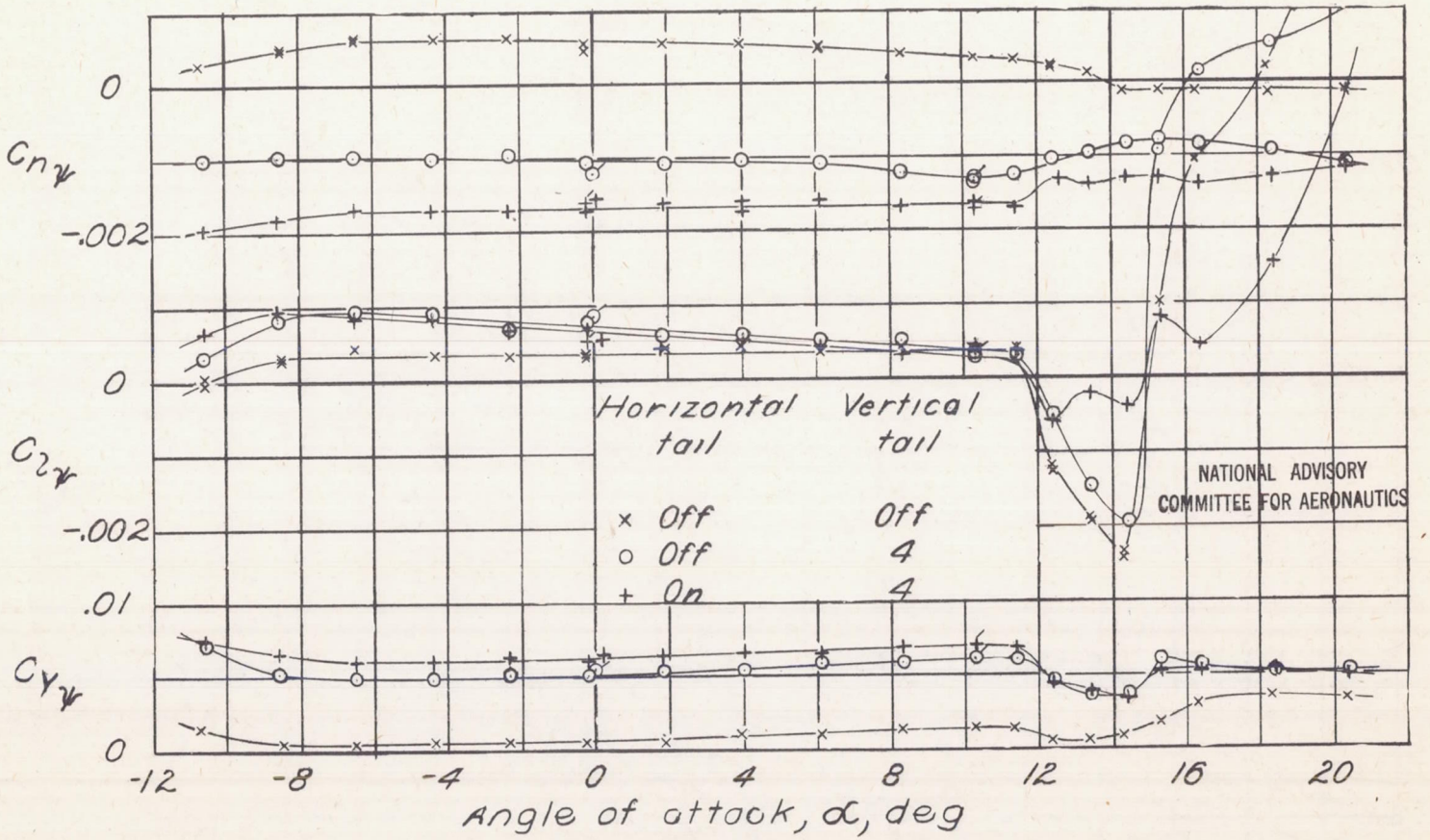

(a) Γ, 0°.

Figure 7.- Effect of horizontal tail surface on variation of lateral-stability slopes C_{n_ψ}, C_{l_ψ}, and C_{Y_ψ} with angle of attack. Short fuselage; q, 65 lb/sq ft.

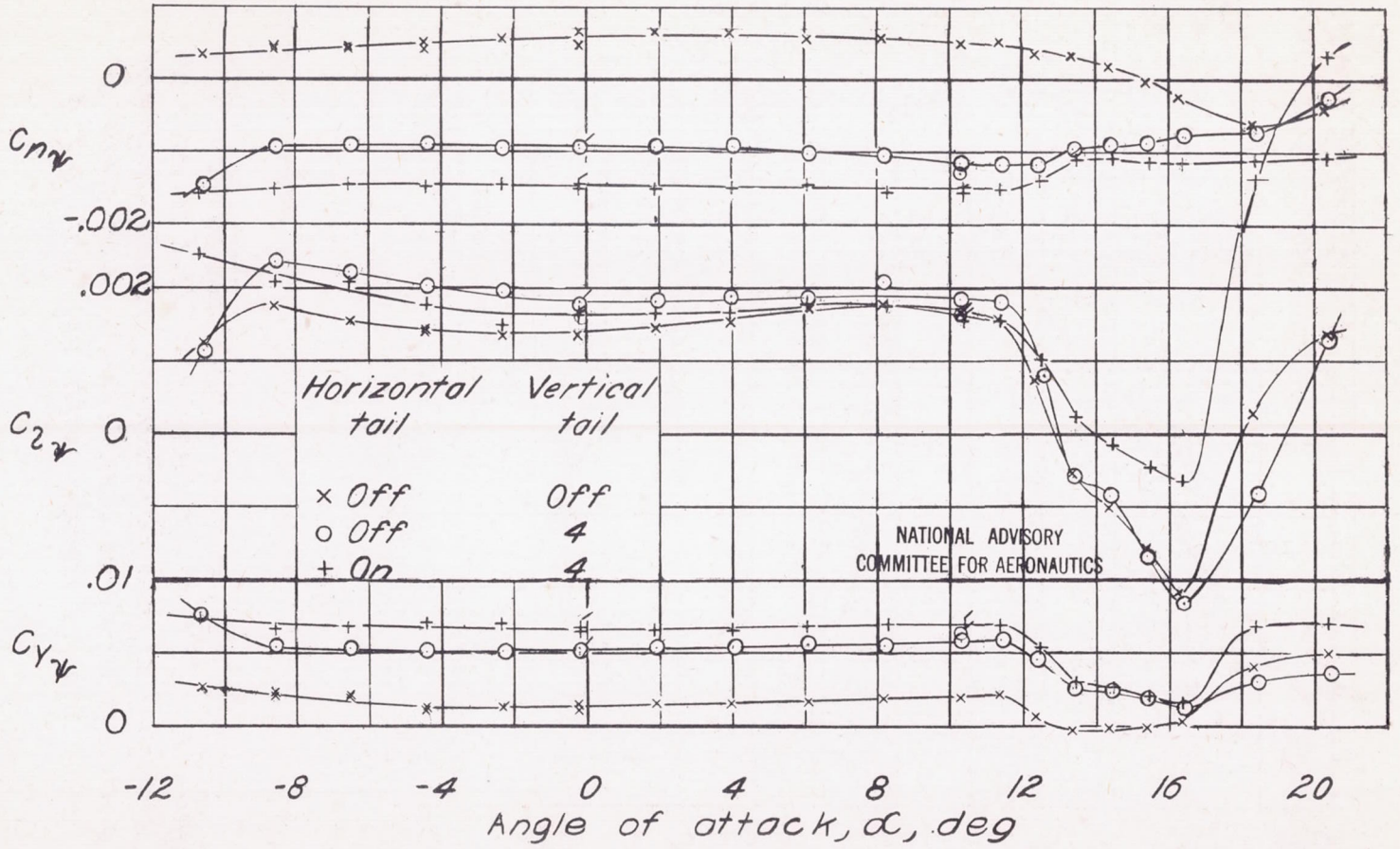

(b) Γ, 5°.

Figure 7.- Concluded.

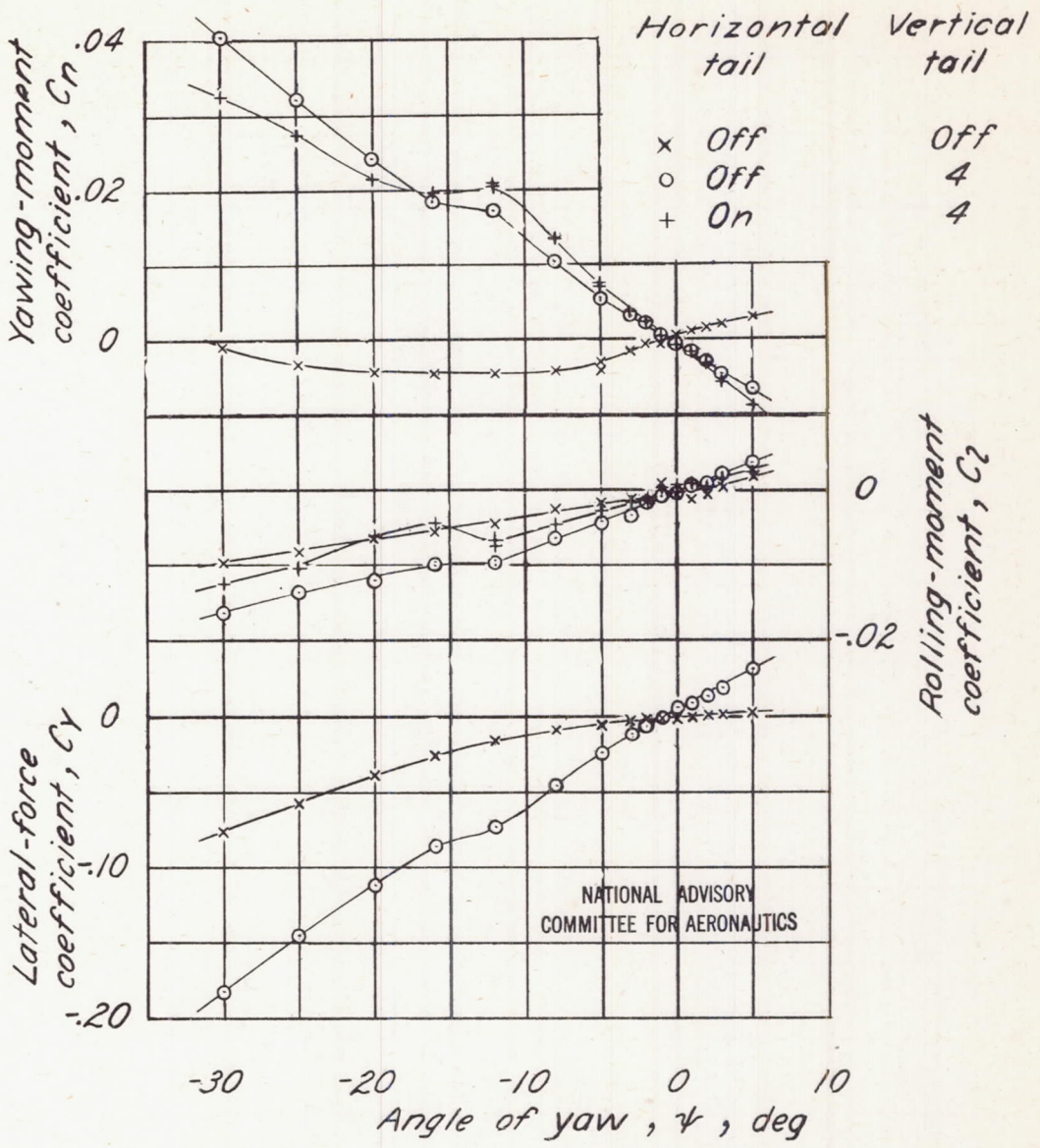

(a) Γ, 0°; α, -0.2°; q, 65 lb/sq ft.

Figure 8.- Effect of horizontal tail surface on variation of yawing-moment, rolling-moment, and lateral-force coefficients with angle of yaw. Short fuselage with vertical tail 4.

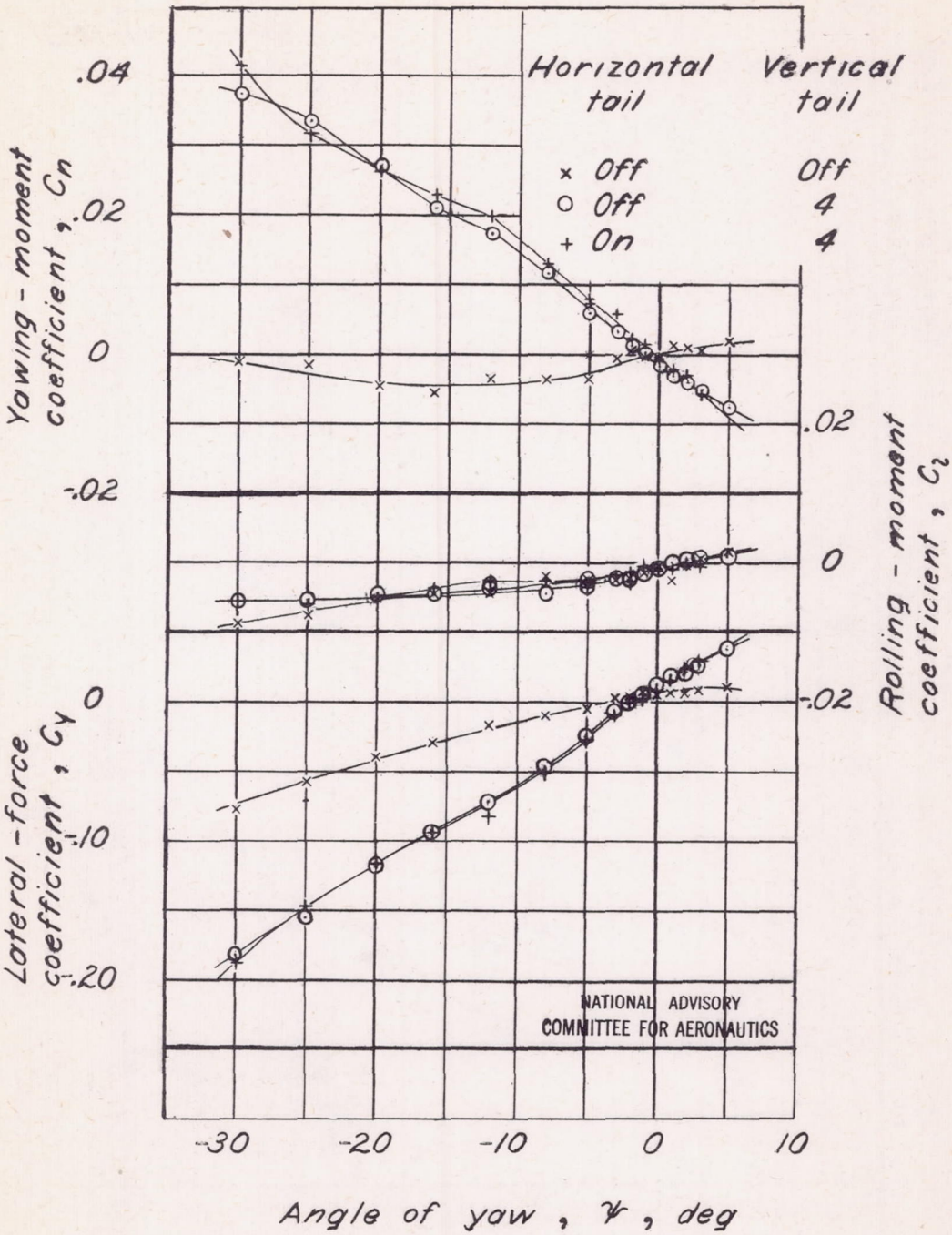

(b) Γ, 0°; α, 10.3°; q, 40 lb/sq ft.

Figure 8.-Continued.

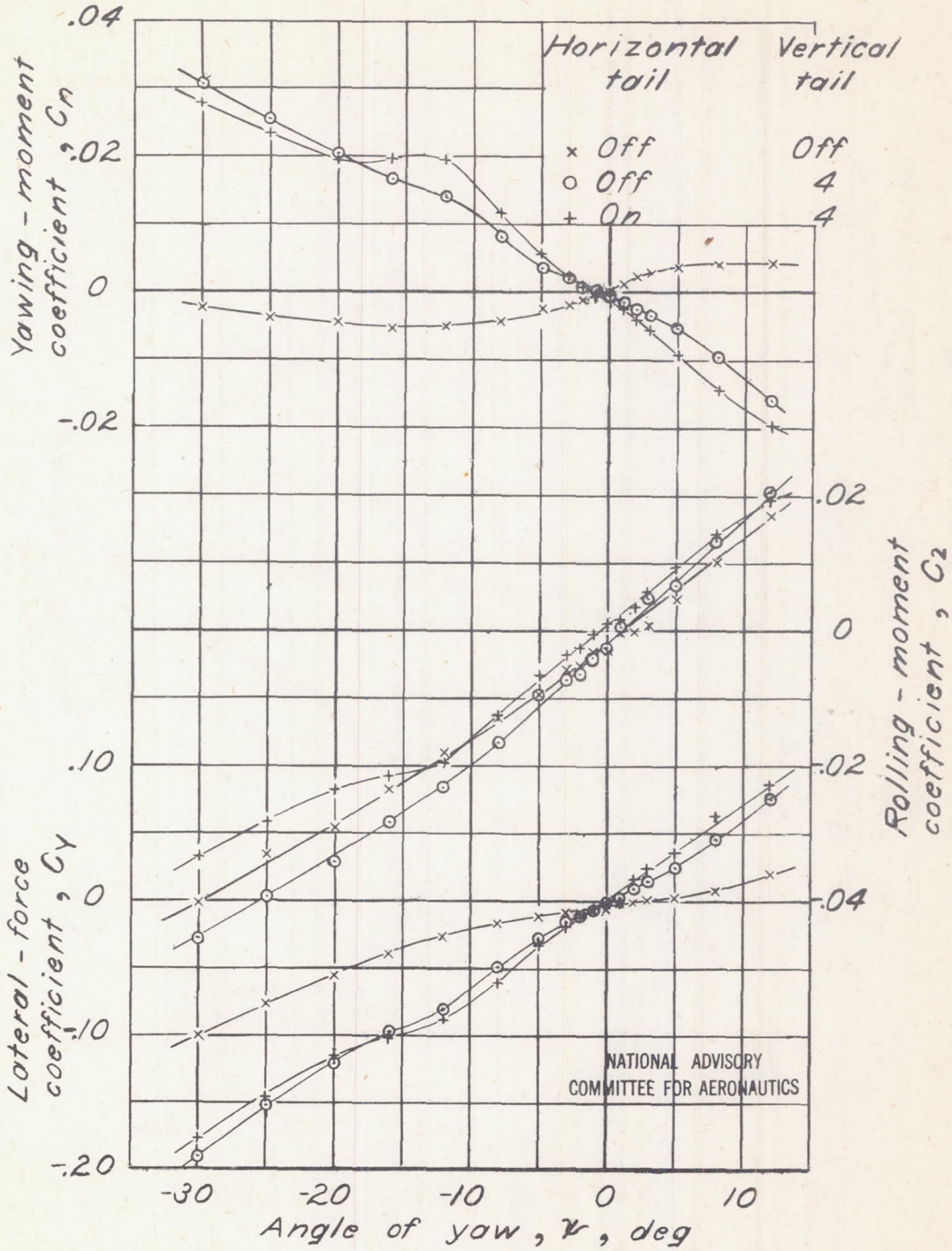

(c) Γ, 5° ; α, -0.2° ; q, 65 lb/sq ft.

Figure 8. - Continued.

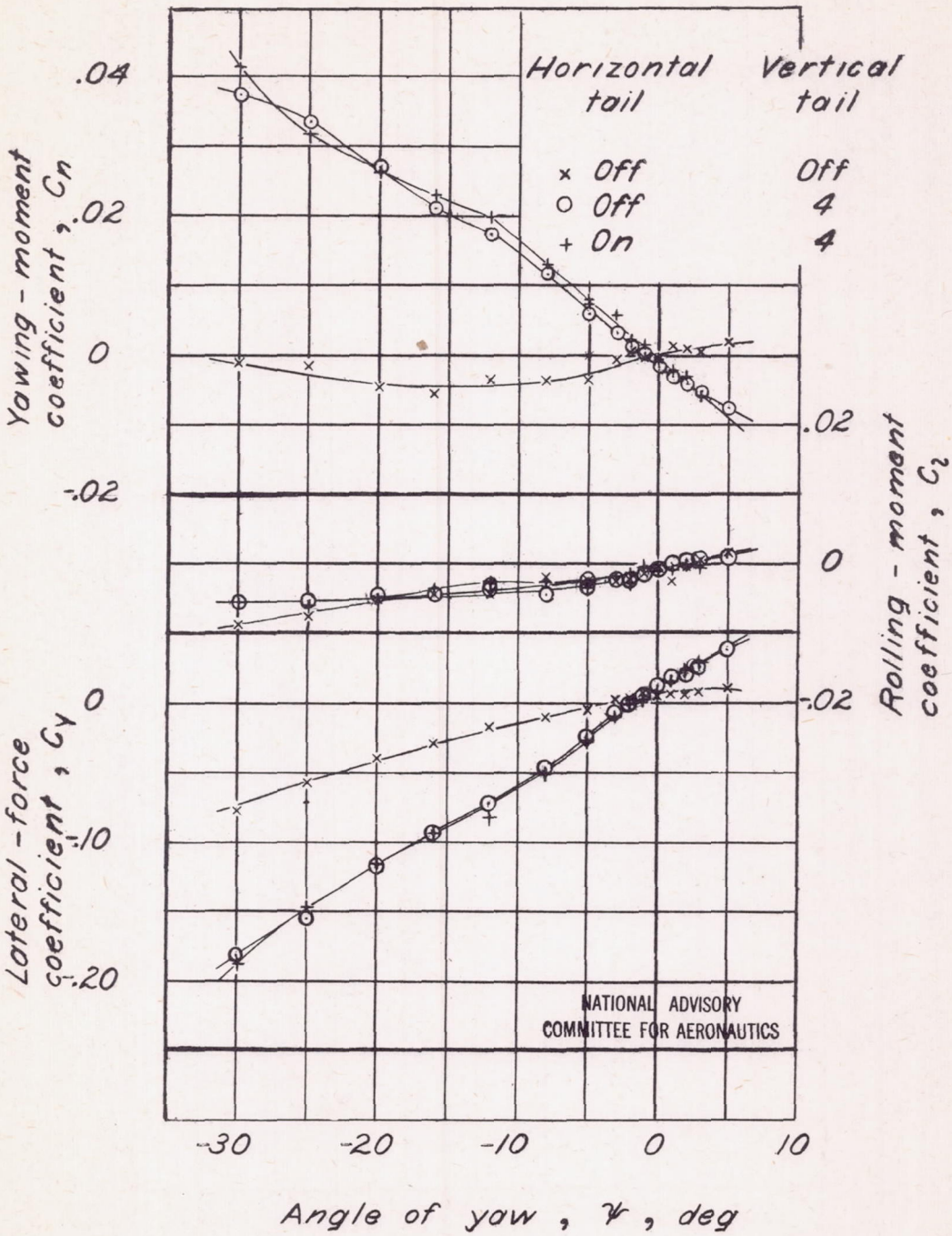

(b) Γ, 0°; α, 10.3°; q, 40 lb/sq ft.

Figure 8.-Continued.

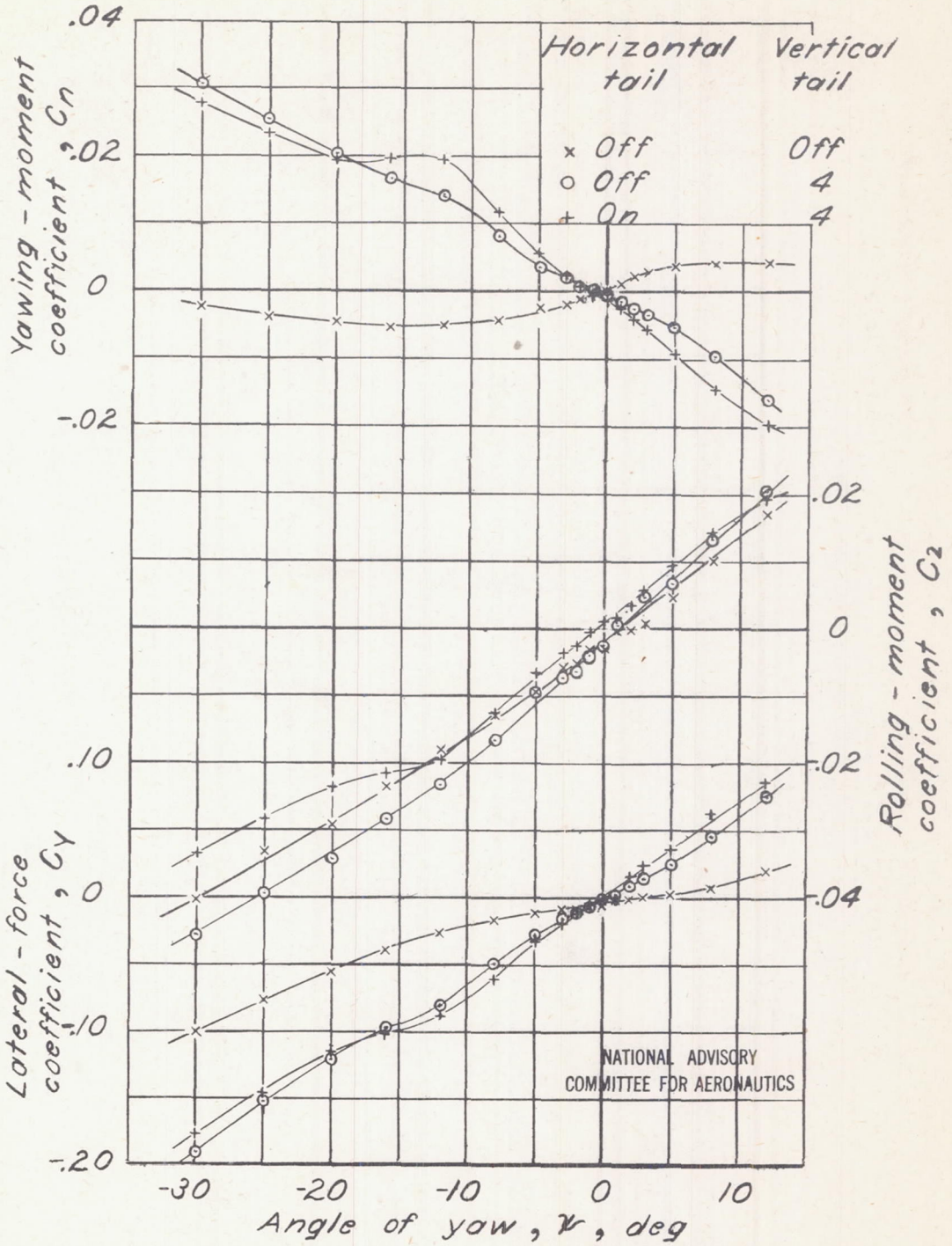

(c) Γ, 5° ; α, -0.2° ; q, 65 lb/sq ft.

Figure 8. - Continued.

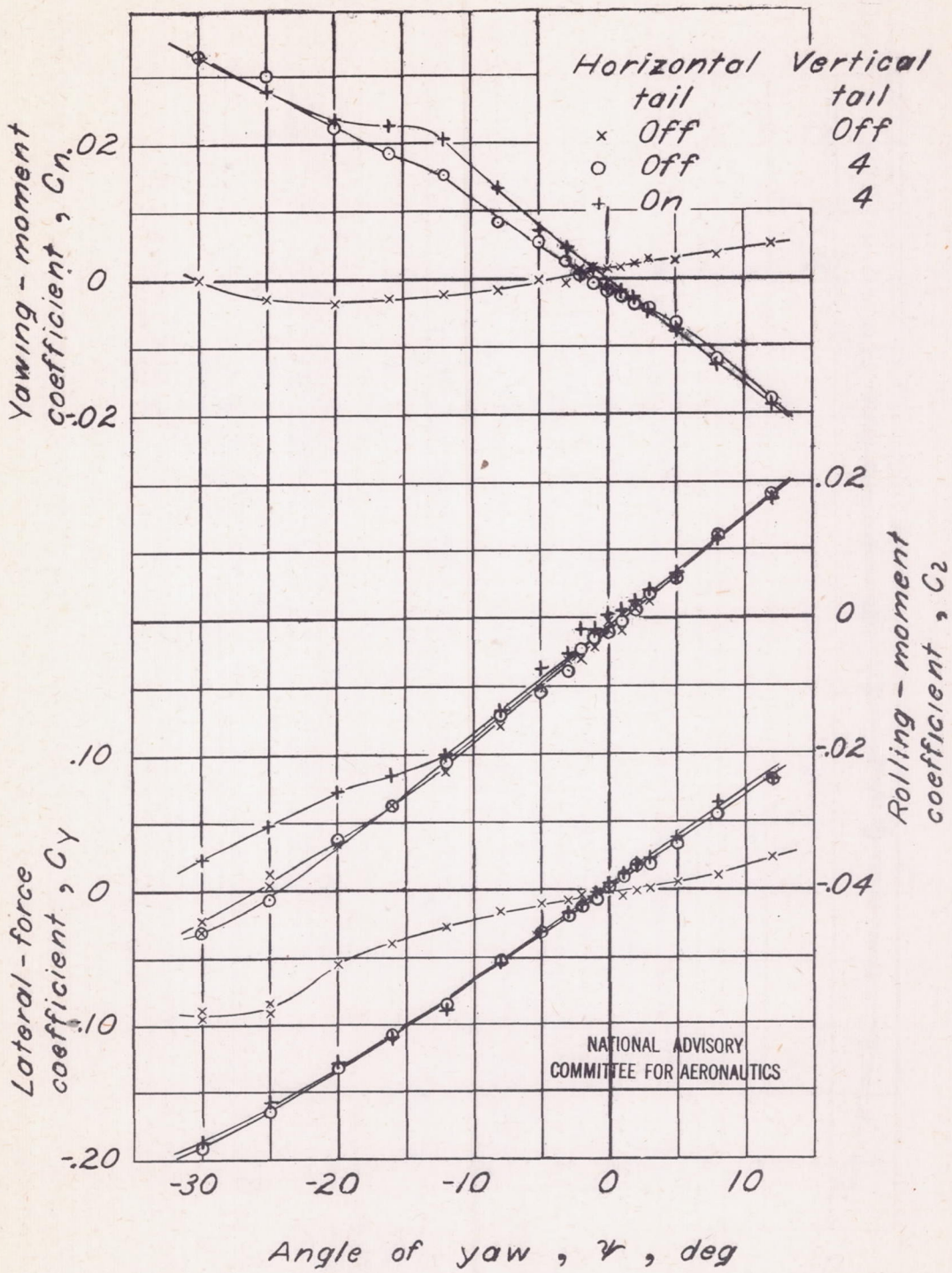

(d) Γ, 5°; α, 10.3°; q, 40 lb/sq ft.

Figure 8. - Concluded.

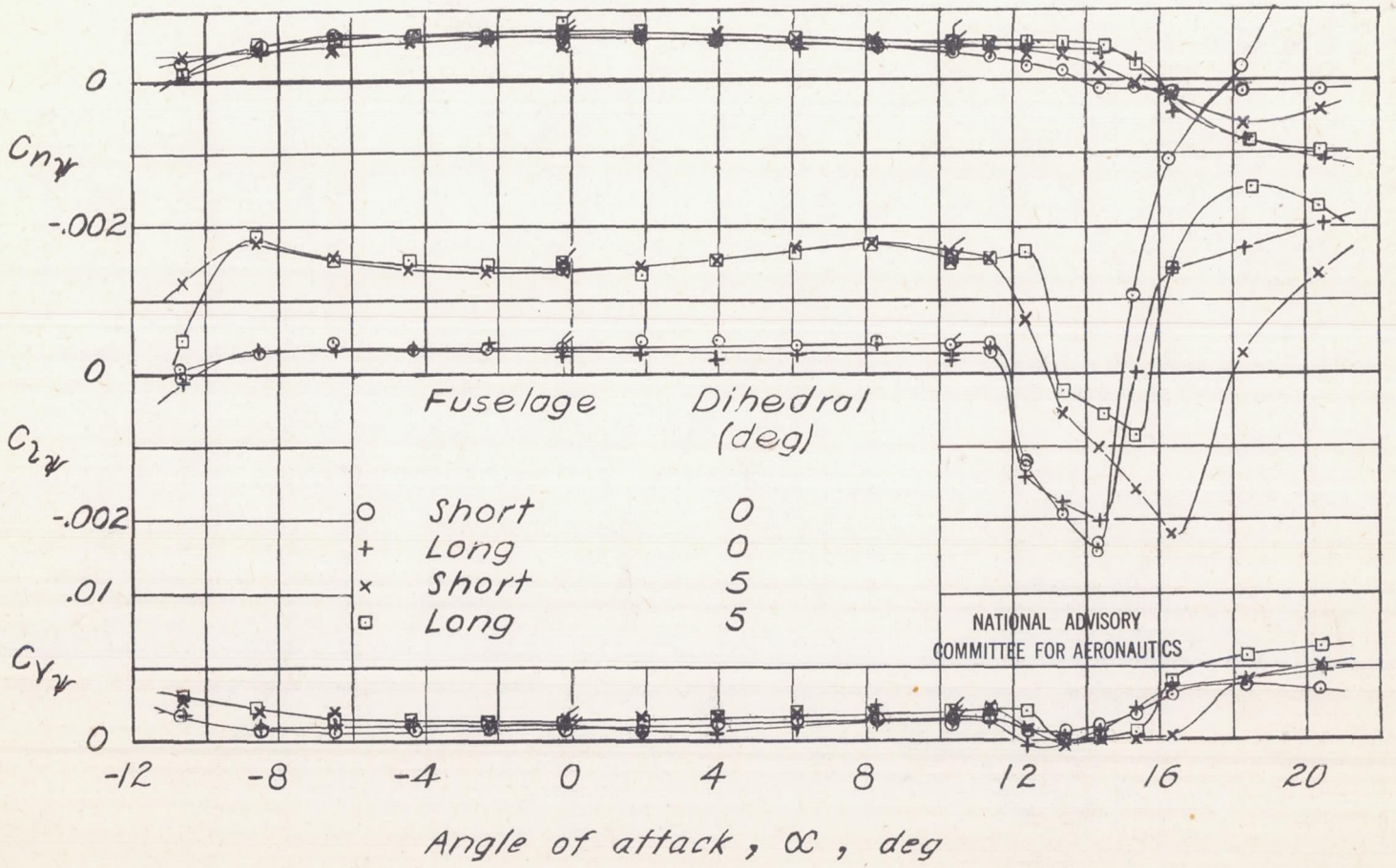

Figure 9 .- Effect of changing fuselage length on variation of lateral-stability slopes C_{n_ψ} , C_{l_ψ} , and C_{Y_ψ} with angle of attack . Horizontal and vertical tails off ; q , 65 lb/sq ft.

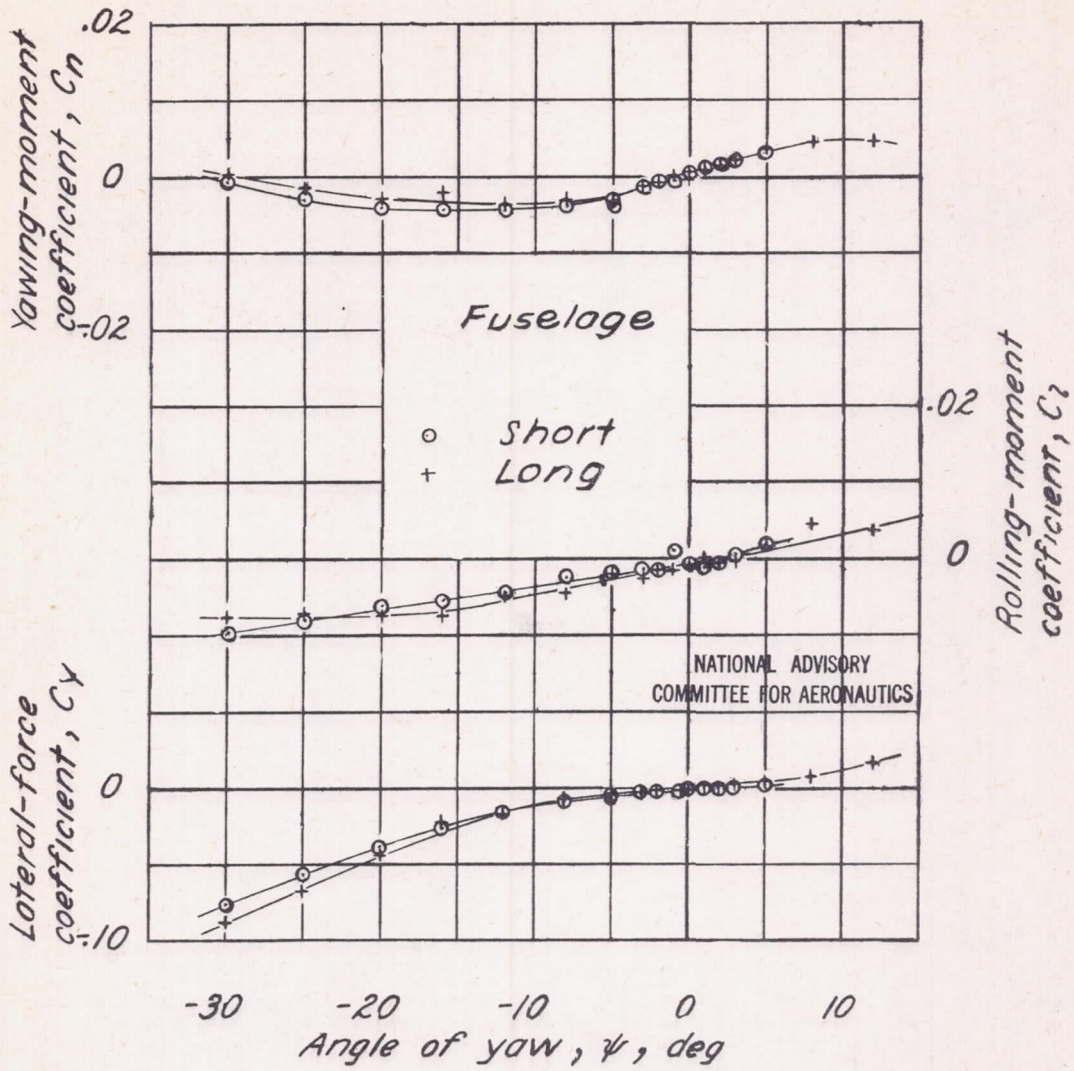

(a) Γ, 0°; α, -0.2°; q, 65 lb/sq ft.

Figure 10.- Effect of changing fuselage length on variation of yawing-moment, rolling-moment, and lateral-force coefficients with angle of yaw. Horizontal and vertical tails off.

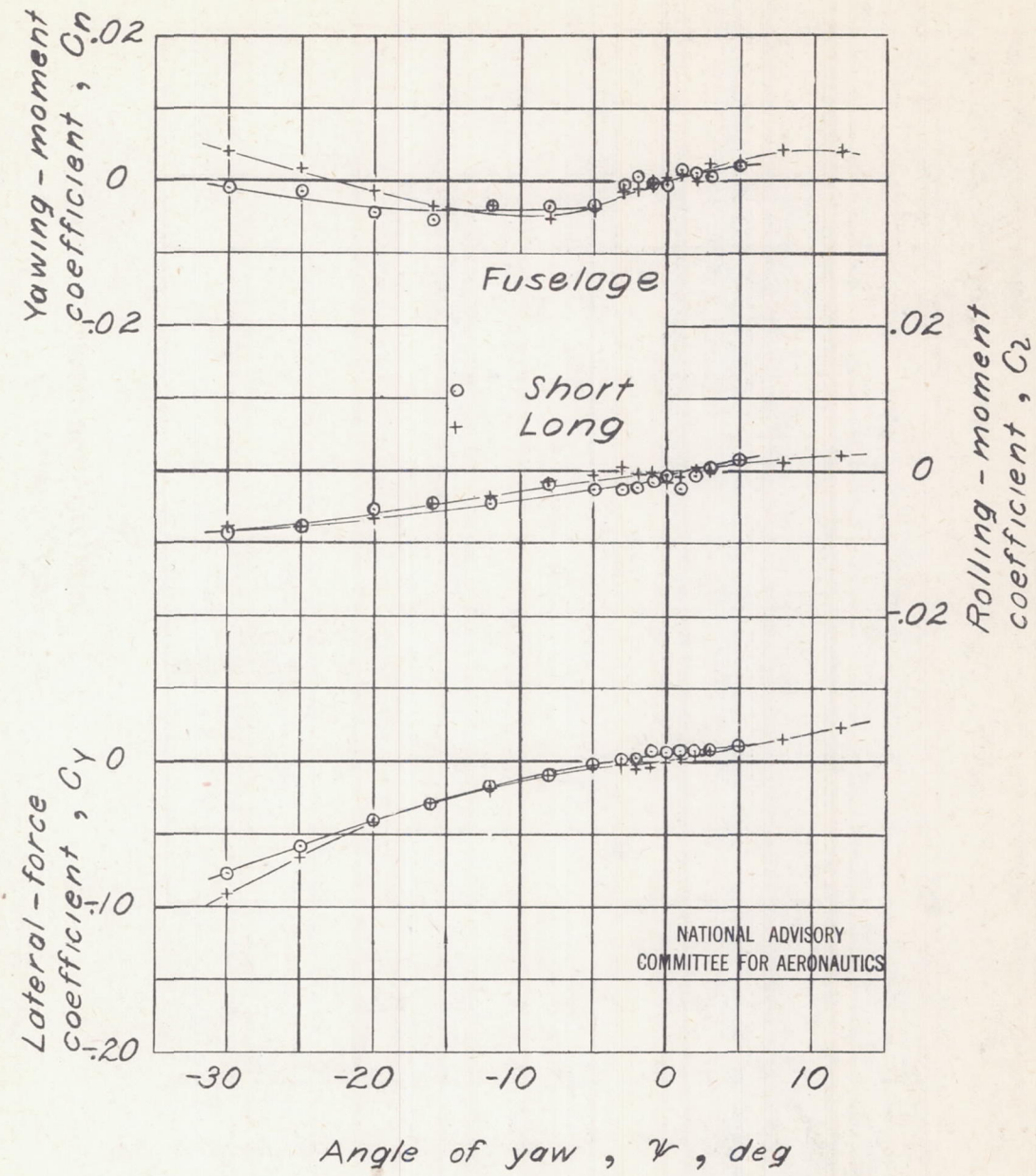

(b) Γ, 0° ; α, 10.3° ; q, 40 lb/sq ft.

Figure 10 .- Continued .

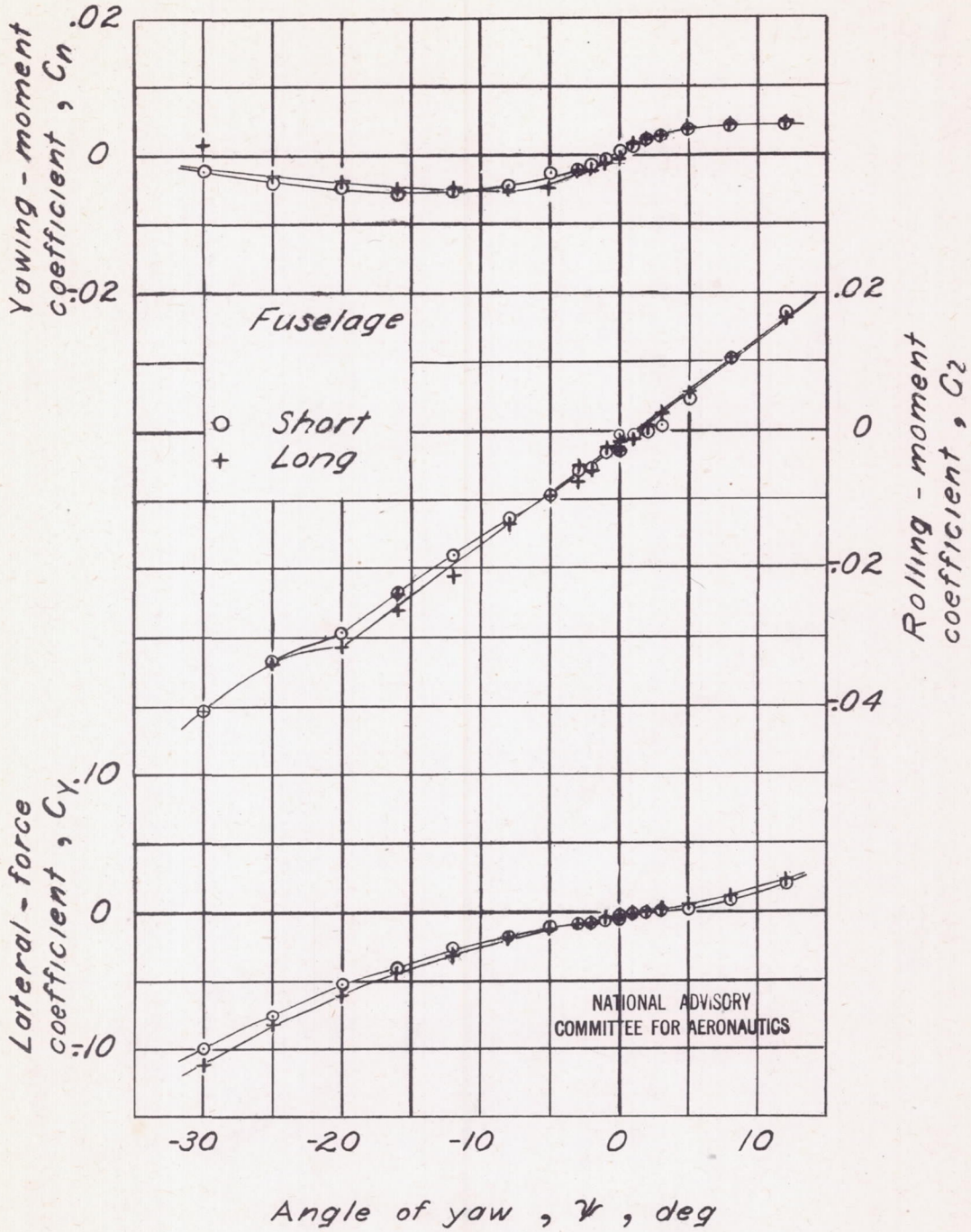

(c) Γ, 5°; α, -0.2°; q, 65 lb/sq ft.

Figure 10.- Continued.

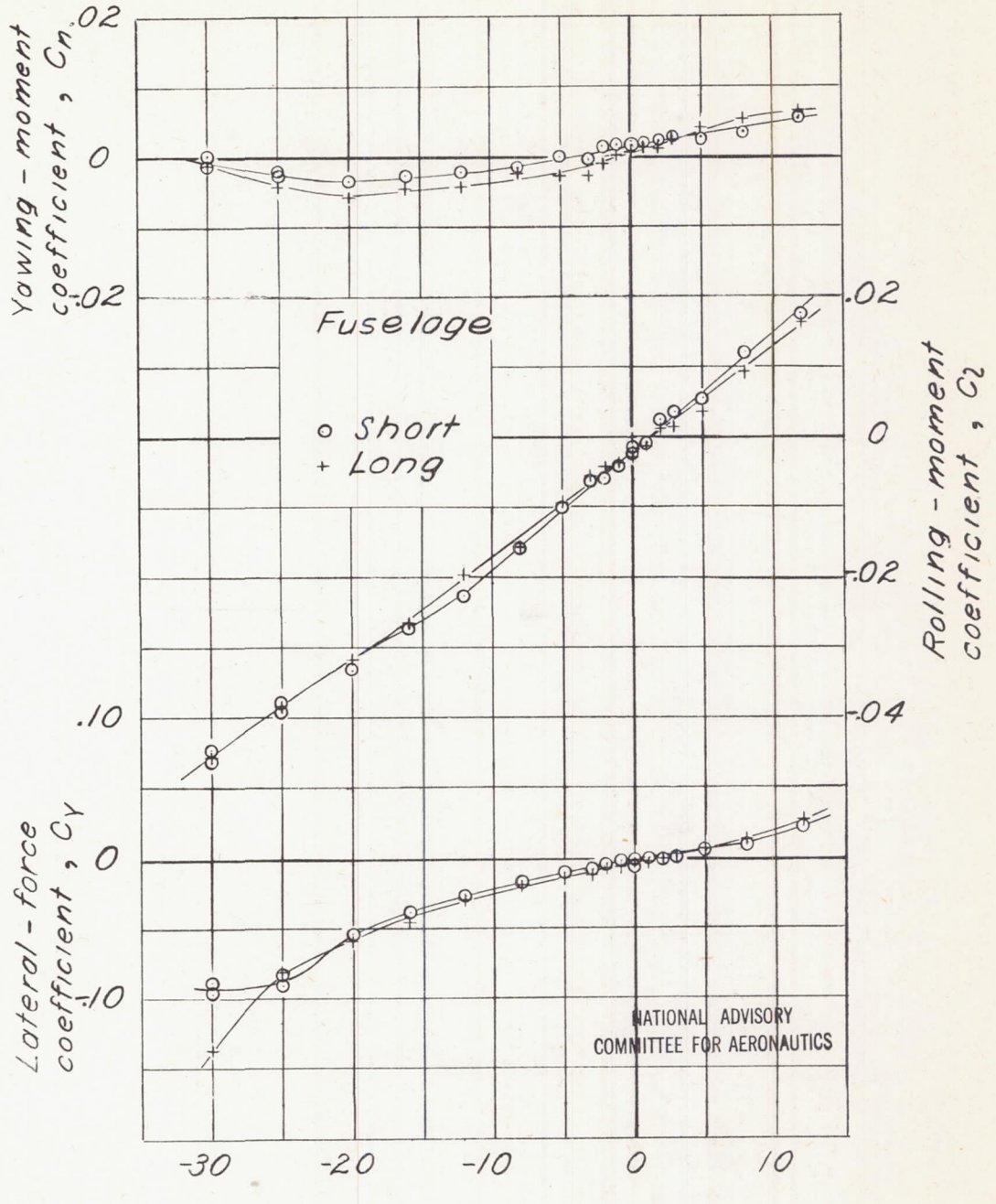

(d) Γ, 5°; α, 10.3°; q, 40 lb/sq ft.

Figure 10.--Concluded.

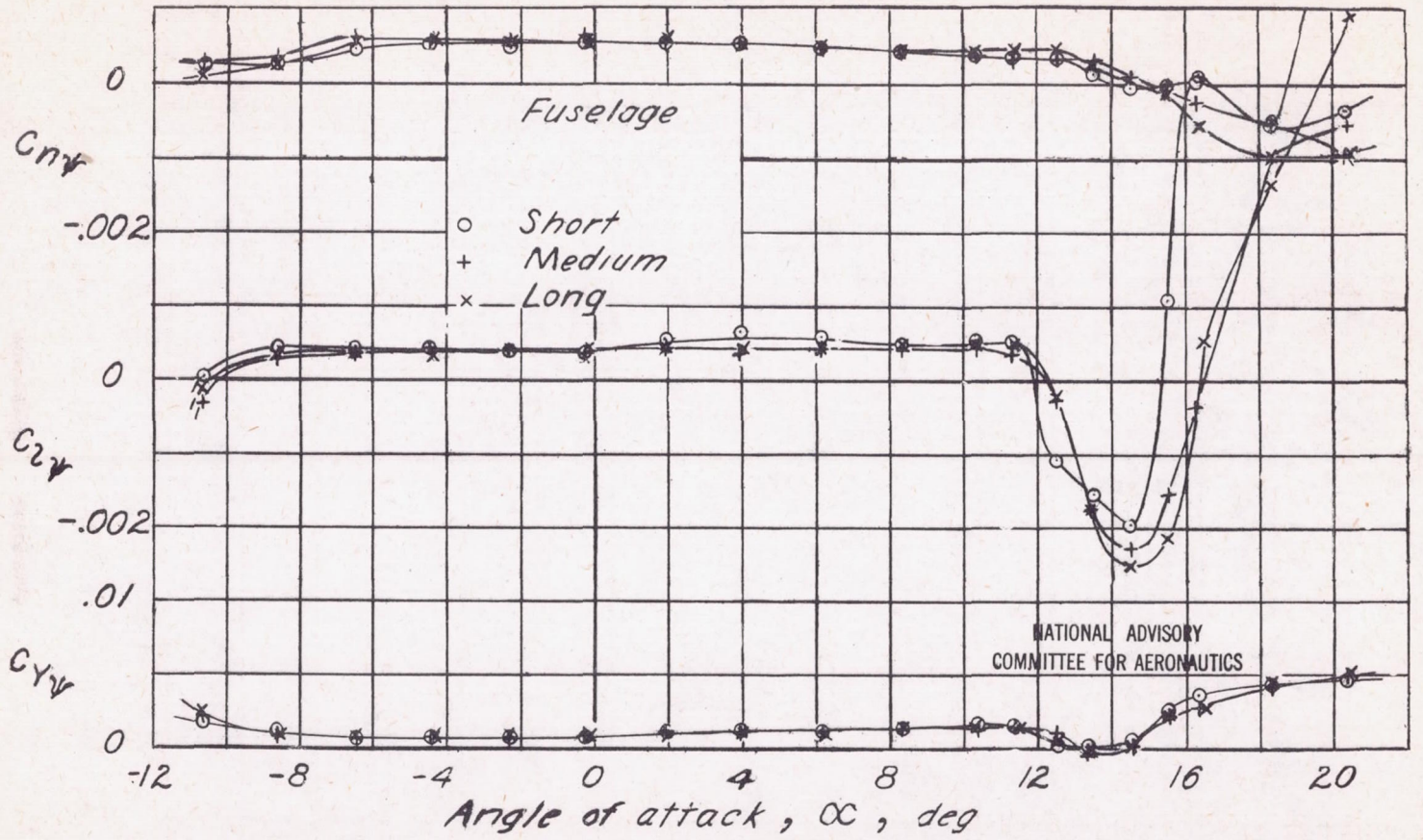

(a) Γ, 0°.

Figure 11.- Effect of changing fuselage length on variation of lateral-stability slopes C_{n_ψ}, C_{l_ψ}, and C_{Y_ψ} with angle of attack. Horizontal tail on; vertical tail off; q, 65 lb/sq ft.

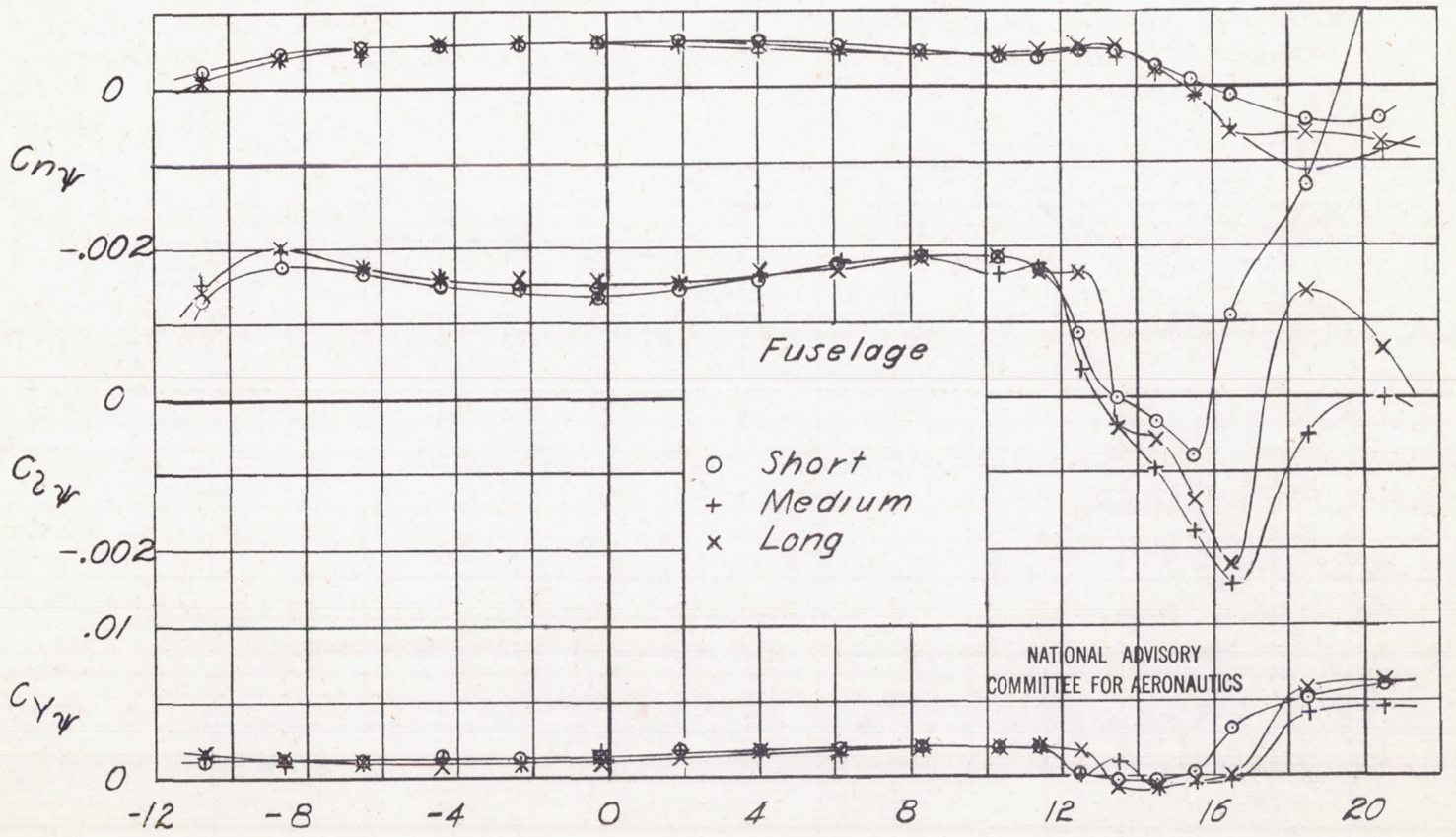

(b) Γ, 5°.

Figure 11.- Concluded.

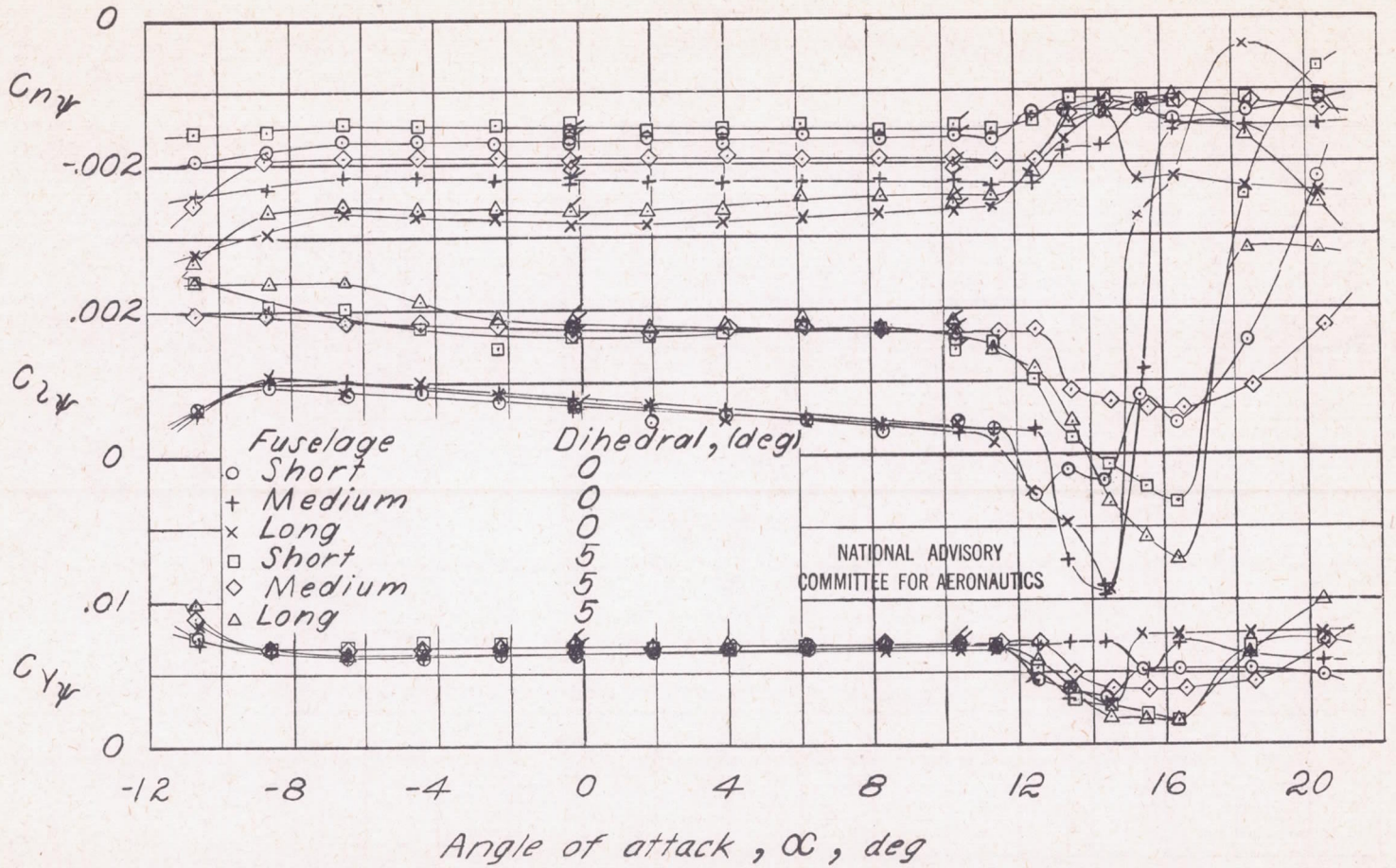

Figure 12.-Effect of changing fuselage length on variation of lateral-stability slopes C_{n_ψ}, C_{l_ψ}, and C_{Y_ψ} with angle of attack. Horizontal tail and vertical tail 4 on; q, 65 lb/sq ft.

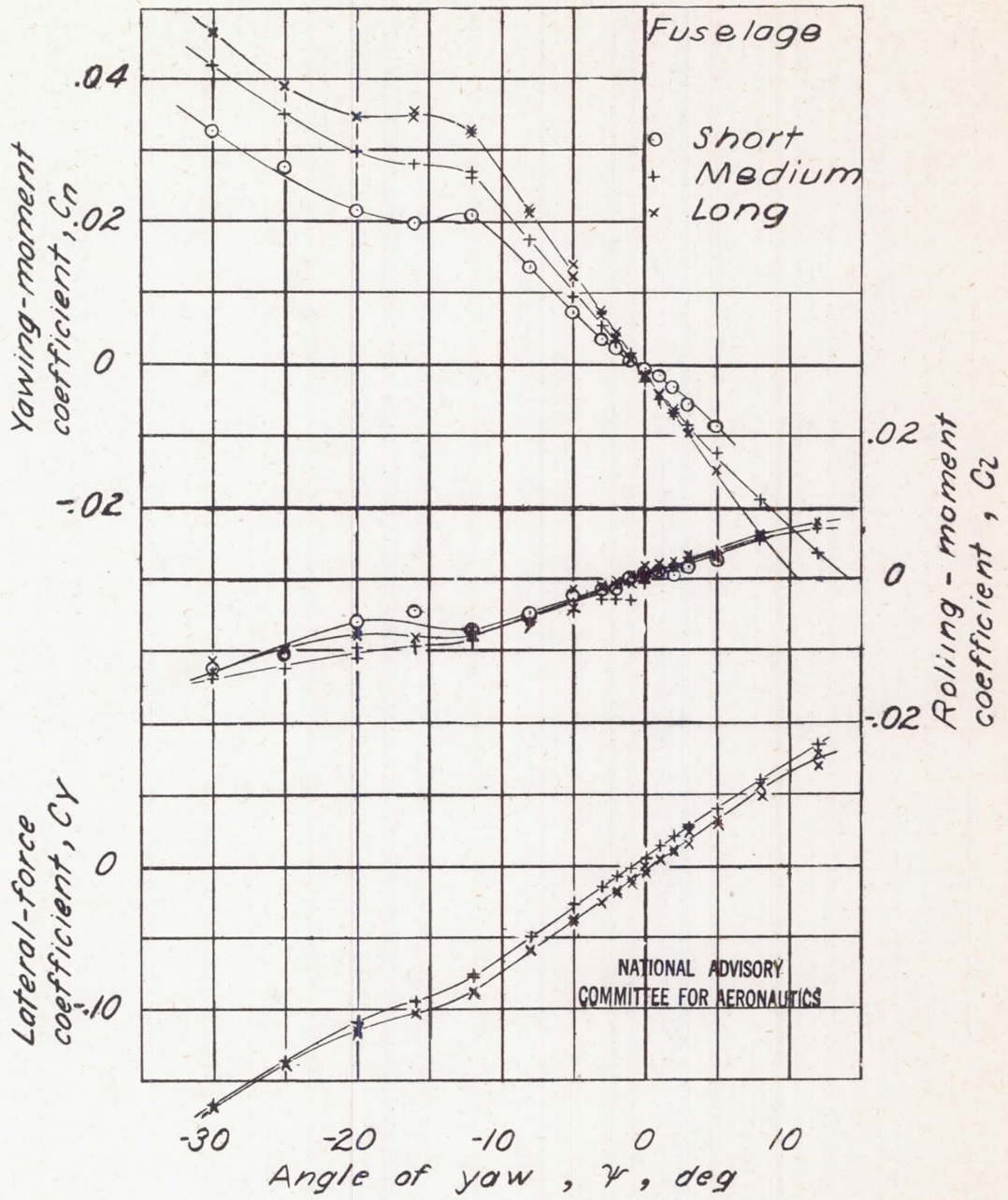

(a) Γ, 0°; α, -0.2°; q, 65 lb/sq ft.

Figure 13.- Effect of changing fuselage length on variation of yawing-moment, rolling-moment, and lateral-force coefficients with angle of yaw. Horizontal tail and vertical tail 4 on.

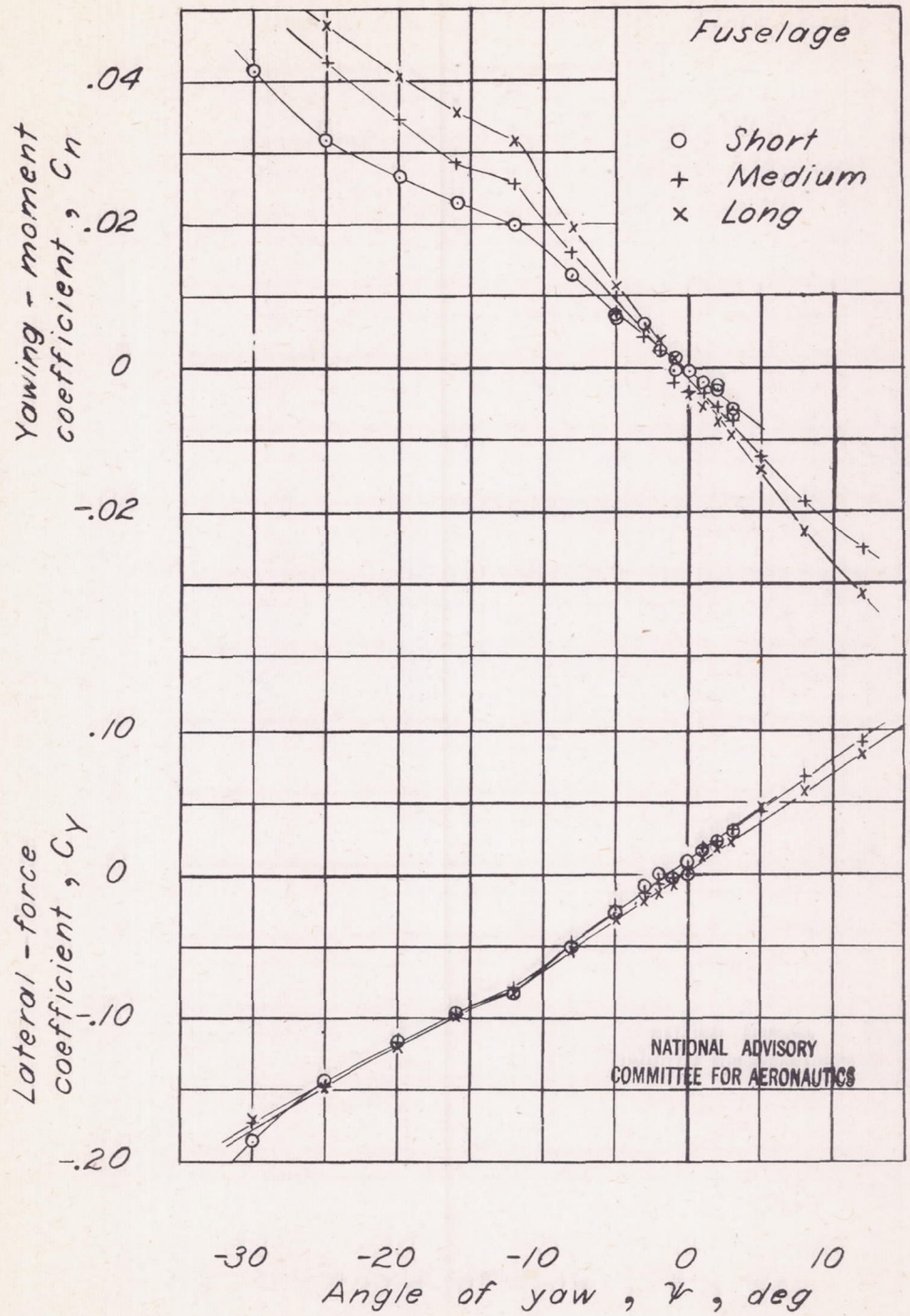

(b) Γ , 0° ; α , 10.3° ; q , 40 lb/sq ft .

Figure 13 . - Continued .

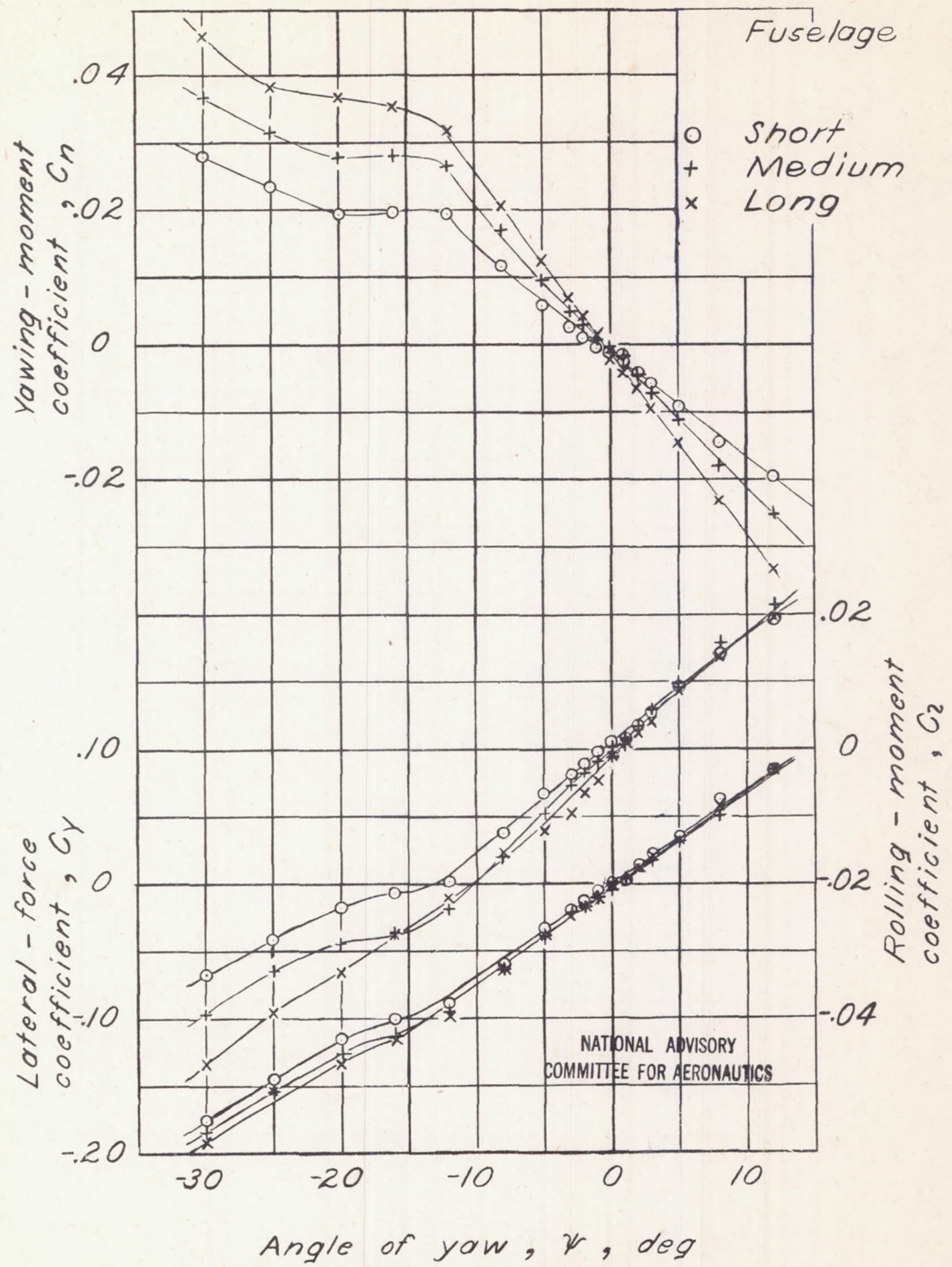

(c) Γ, 5° ; α, -0.2° ; q, 65 lb/sq ft.

Figure 13. - Continued.

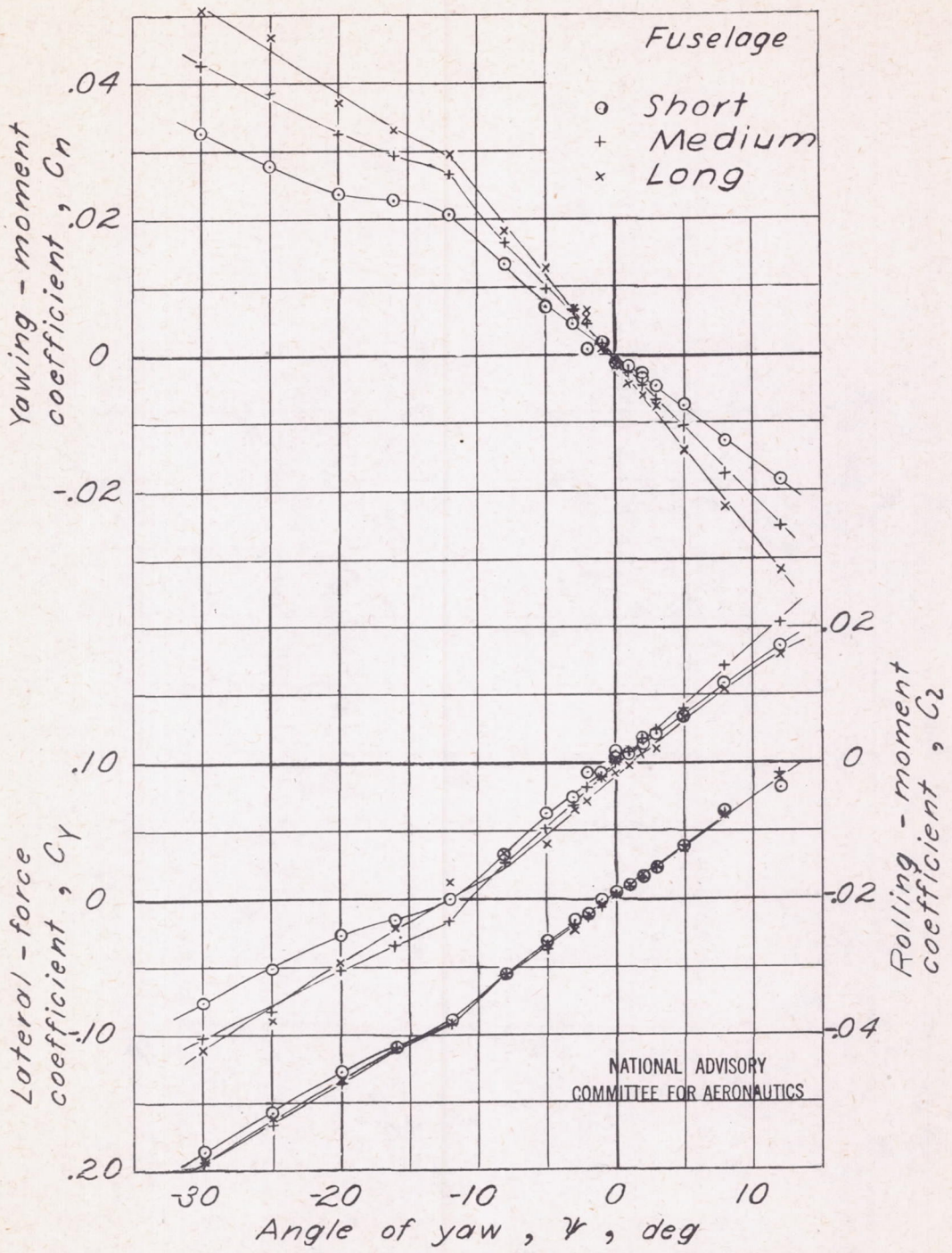

(d) Γ, 5°; α, 10.3°; q, 40 lb/sq ft.

Figure 13. - Concluded.

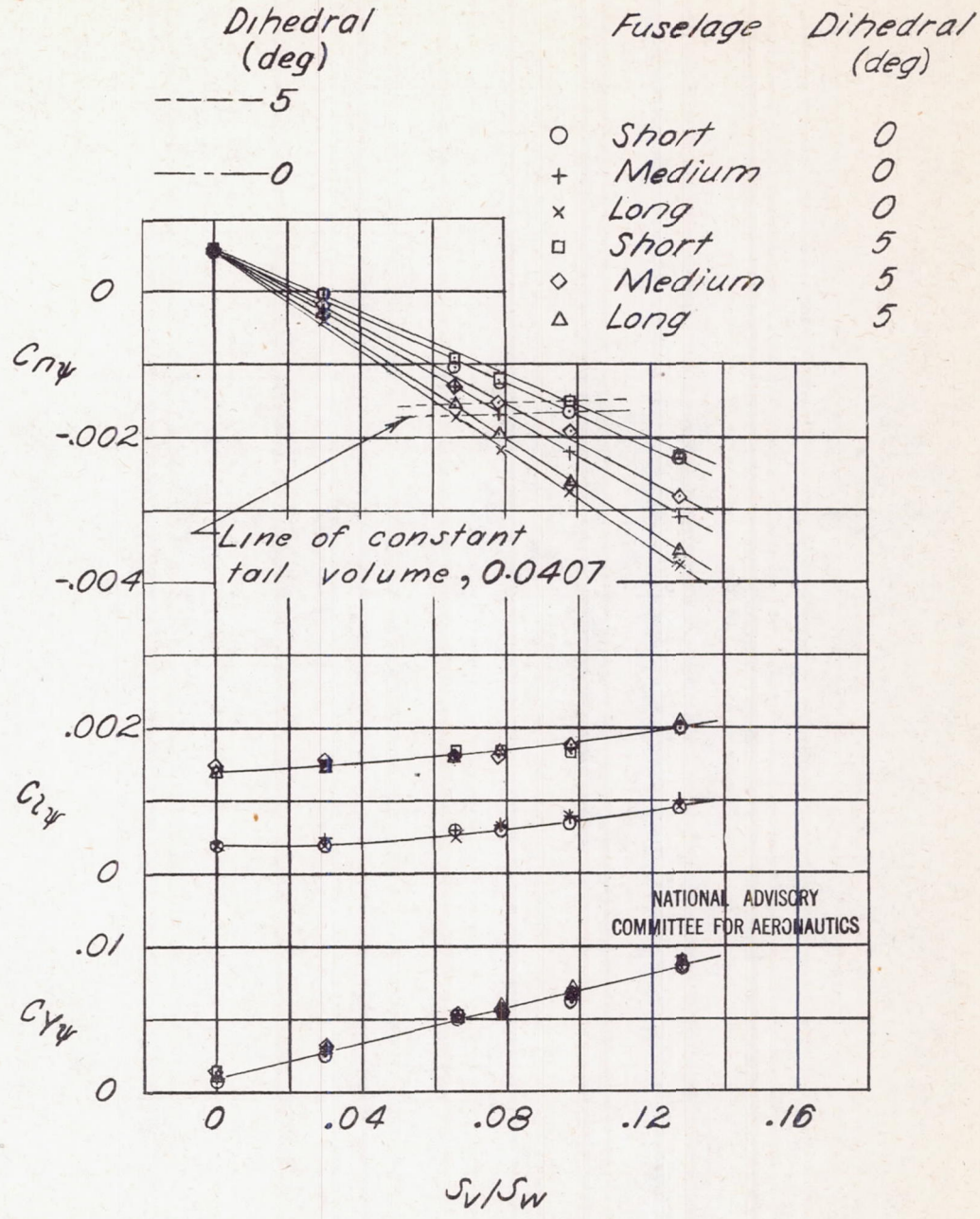

(a) α, 0°.

Figure 14.- Effect of changing fuselage length on variation of lateral-stability slopes C_{n_ψ}, C_{l_ψ}, and C_{y_ψ} with vertical-tail area. Horizontal tail on ; q, 65 lb/sq ft.

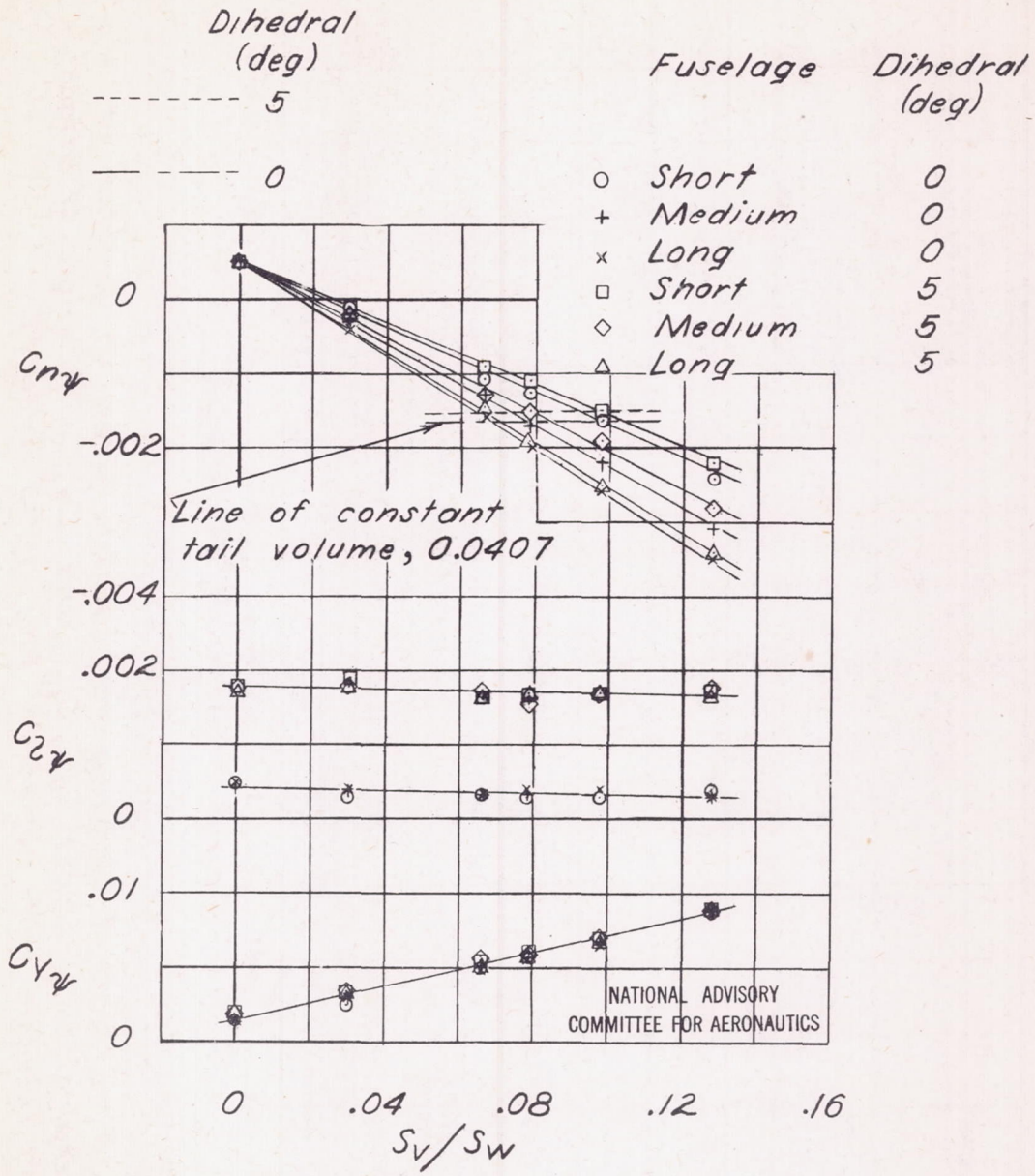

(b) α, 10°.

Figure 14. - Concluded.

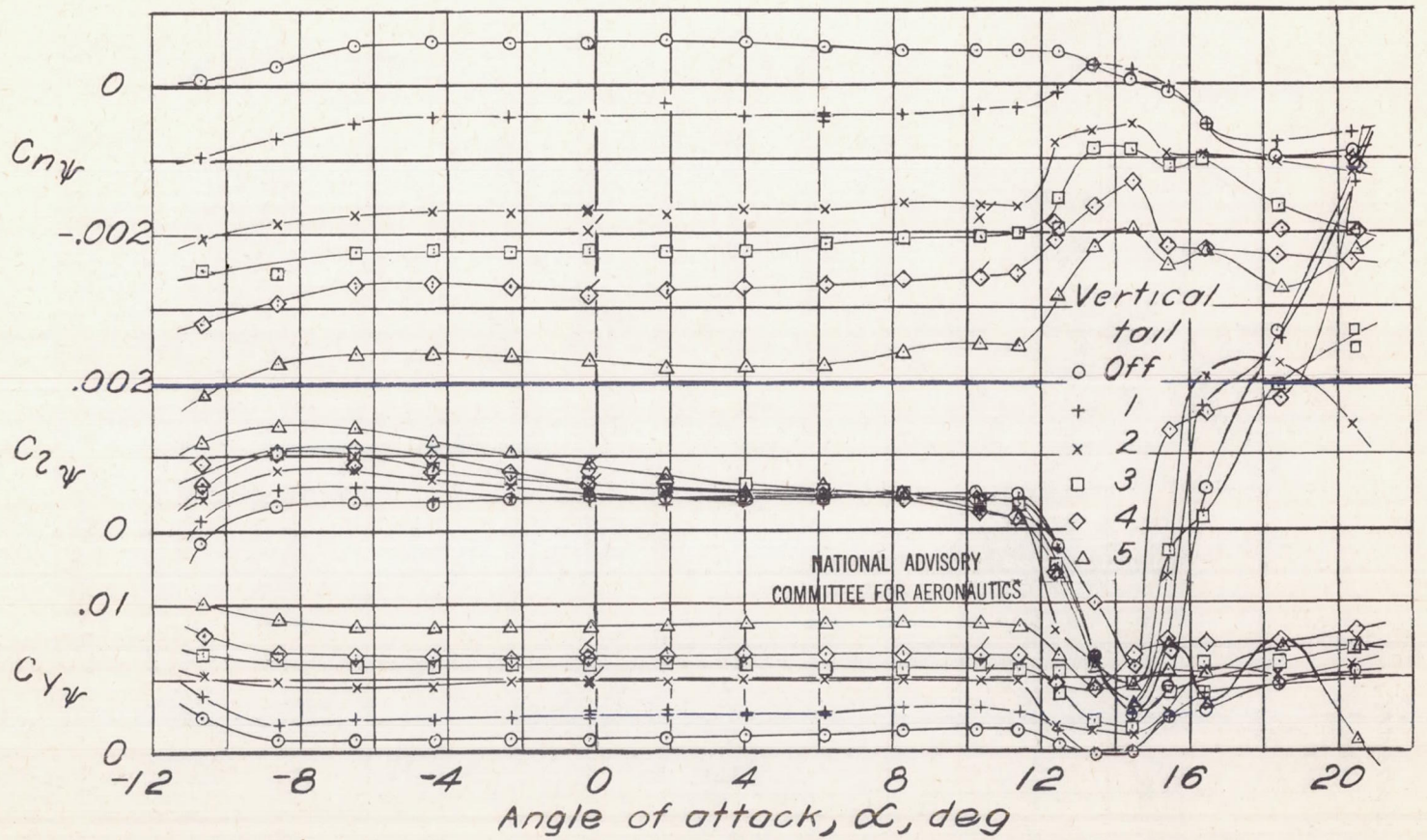

(a) Γ, 0°.

Figure 15.- Effect of changing vertical-tail area on variation of lateral-stability slopes C_{n_ψ}, C_{l_ψ}, and C_{Y_ψ} with angle of attack. Long fuselage with horizontal tail; q, 65 lb/sq ft.

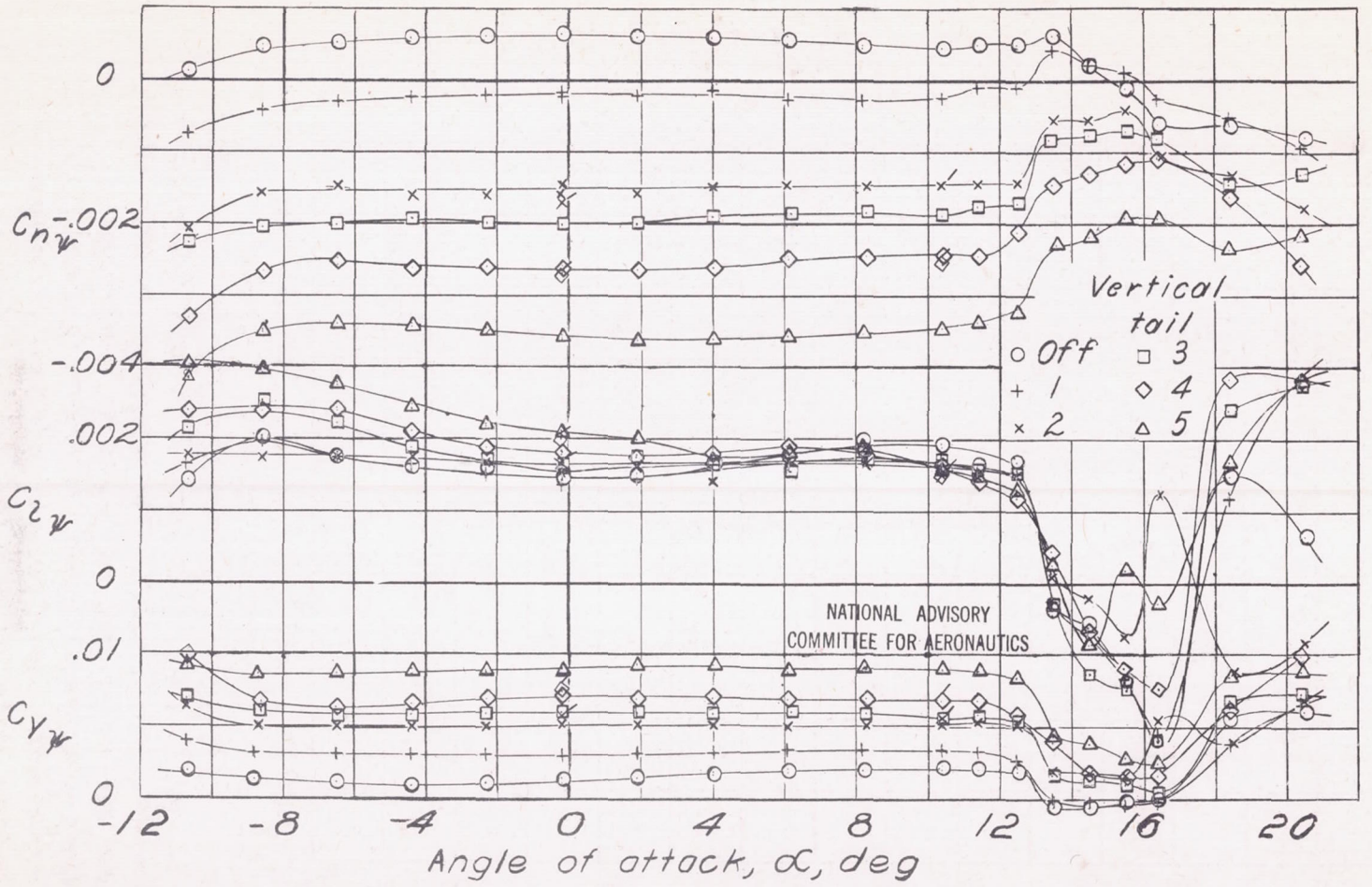

(b) Γ, 5°.

Figure 15.- Concluded.

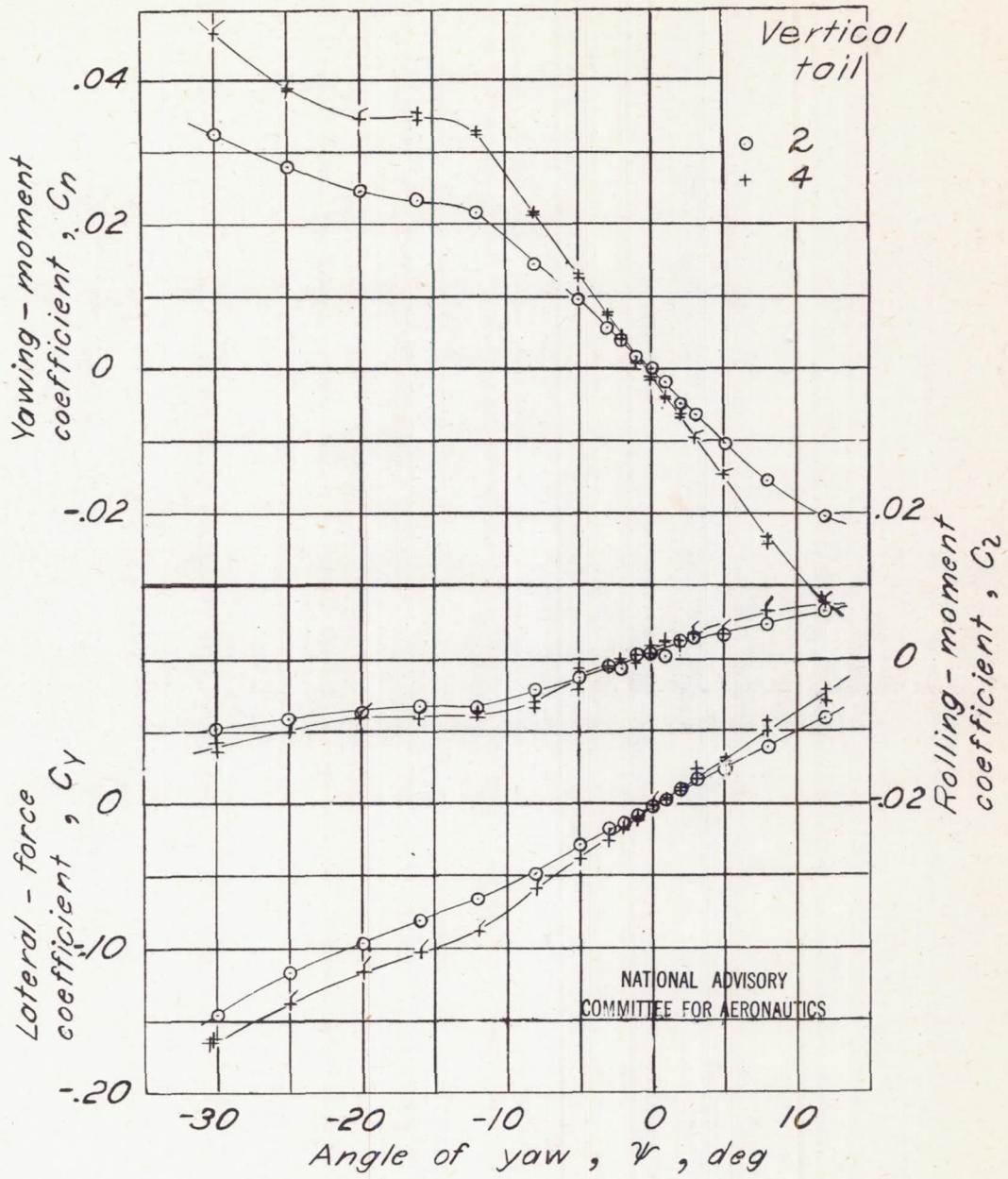

(a) Γ, 0°; α, -0.2°; q, 65 lb/sq ft.

Figure 16. - Effect of changing vertical-tail area on variation of yawing-moment, rolling-moment, and lateral-force coefficients with angle of yaw. Long fuselage with horizontal tail.

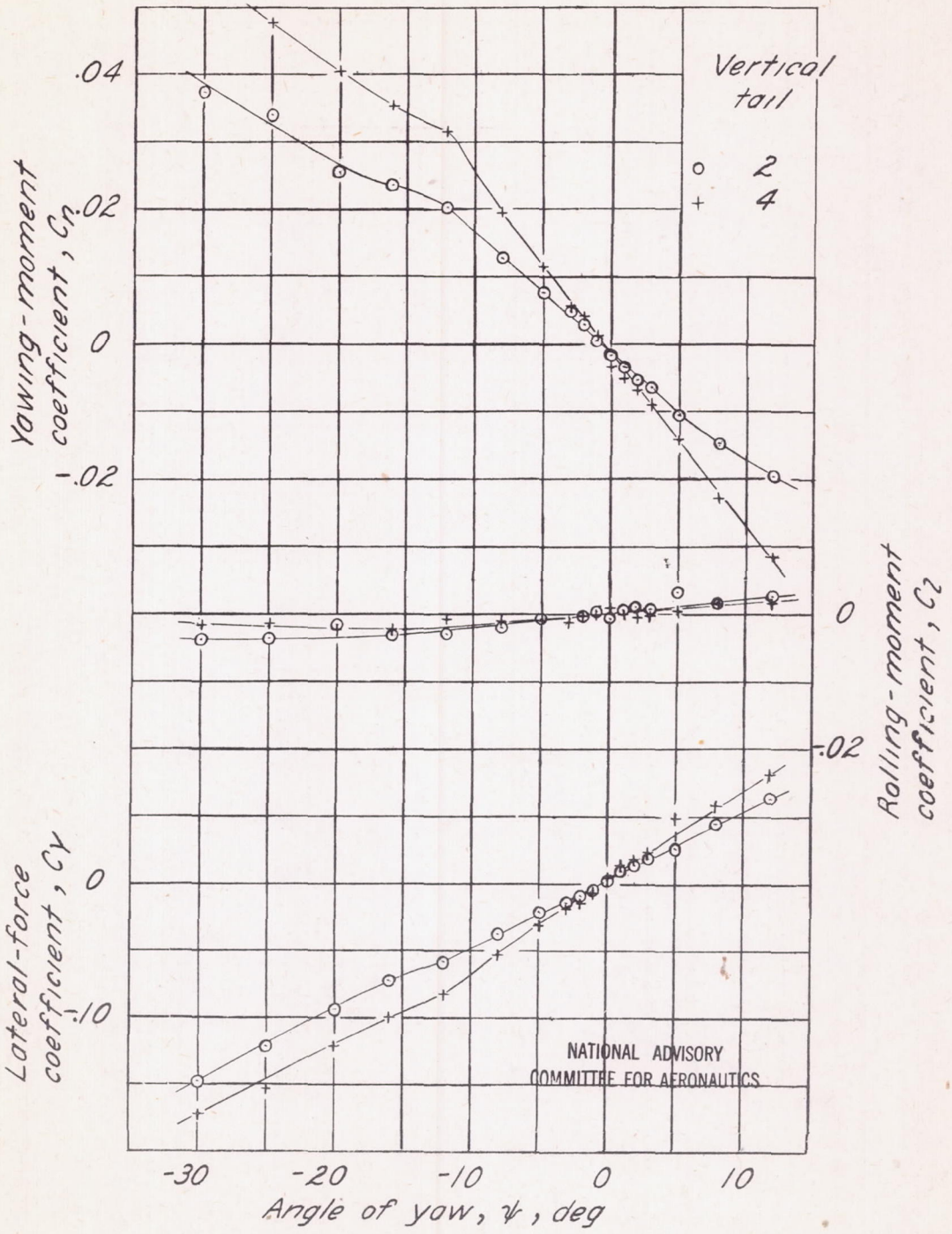

(b) Γ, 0°; α, 10.4°; q, 40 lb/sq ft.

Figure 16.- Continued.

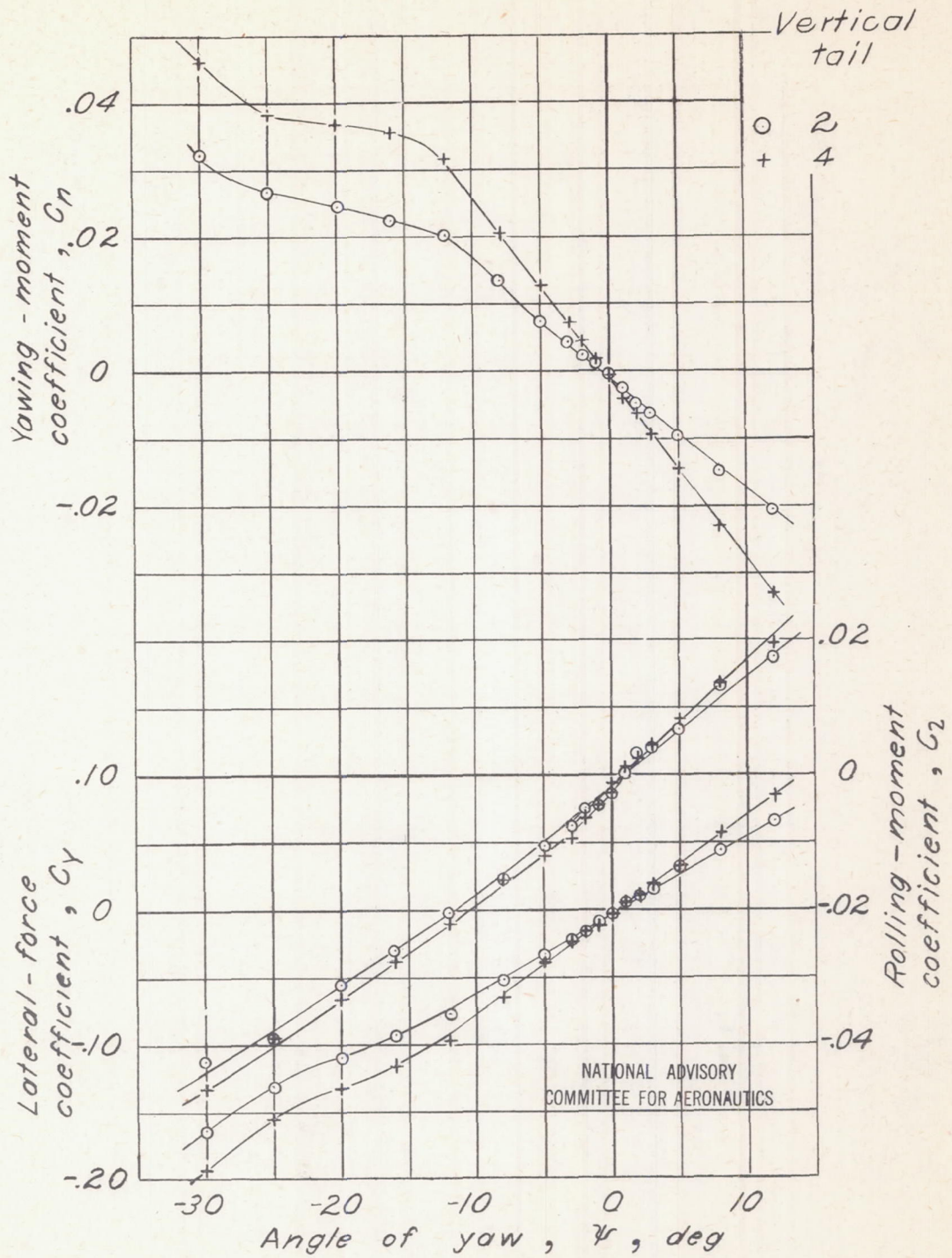

(c) Γ, 5° ; α, -0.2° ; q , 65 lb/sq ft .

Figure 16 . - Continued .

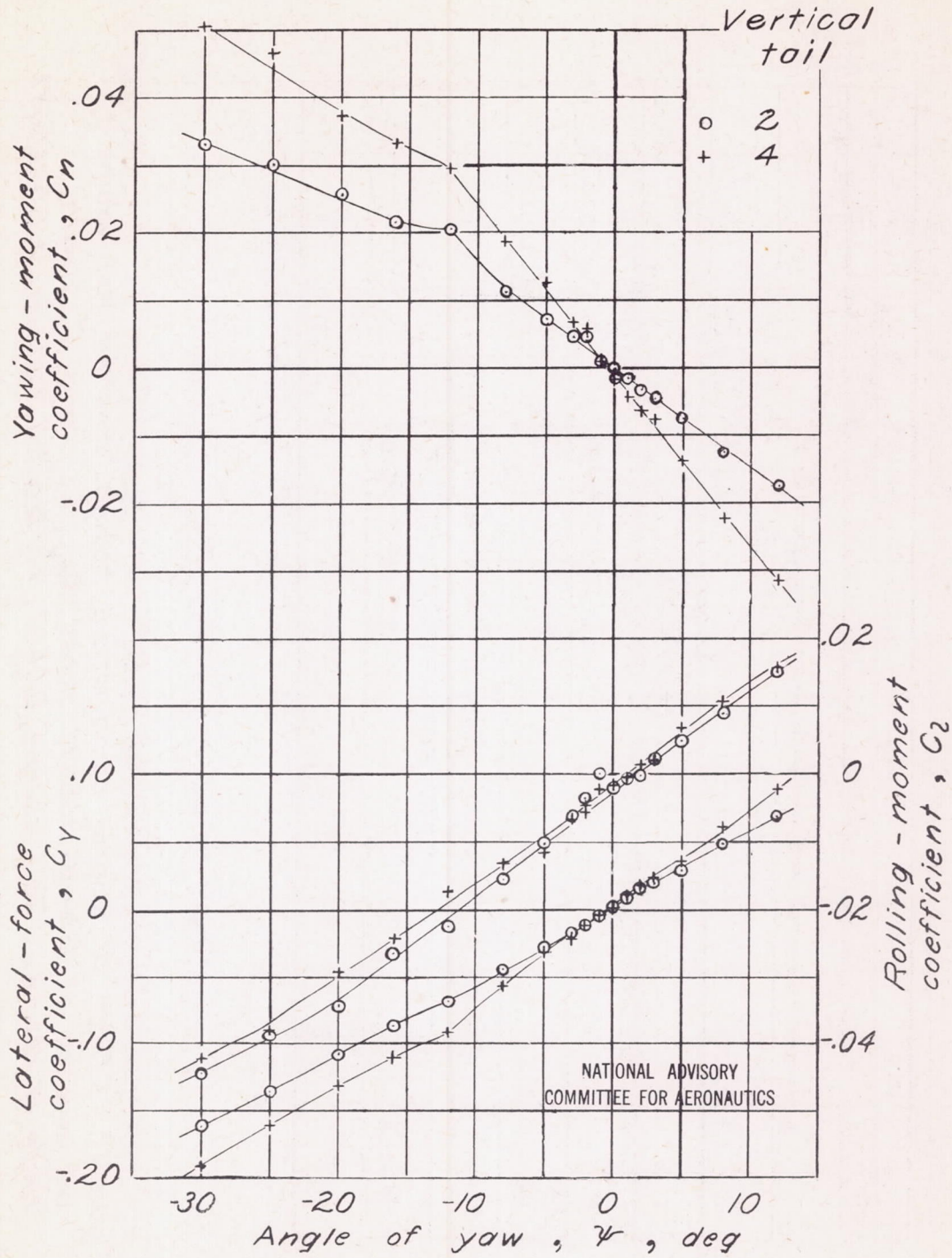

(d) Γ, 5°; α, 10.4°; q, 40 lb/sq ft.

Figure 16. - Concluded.

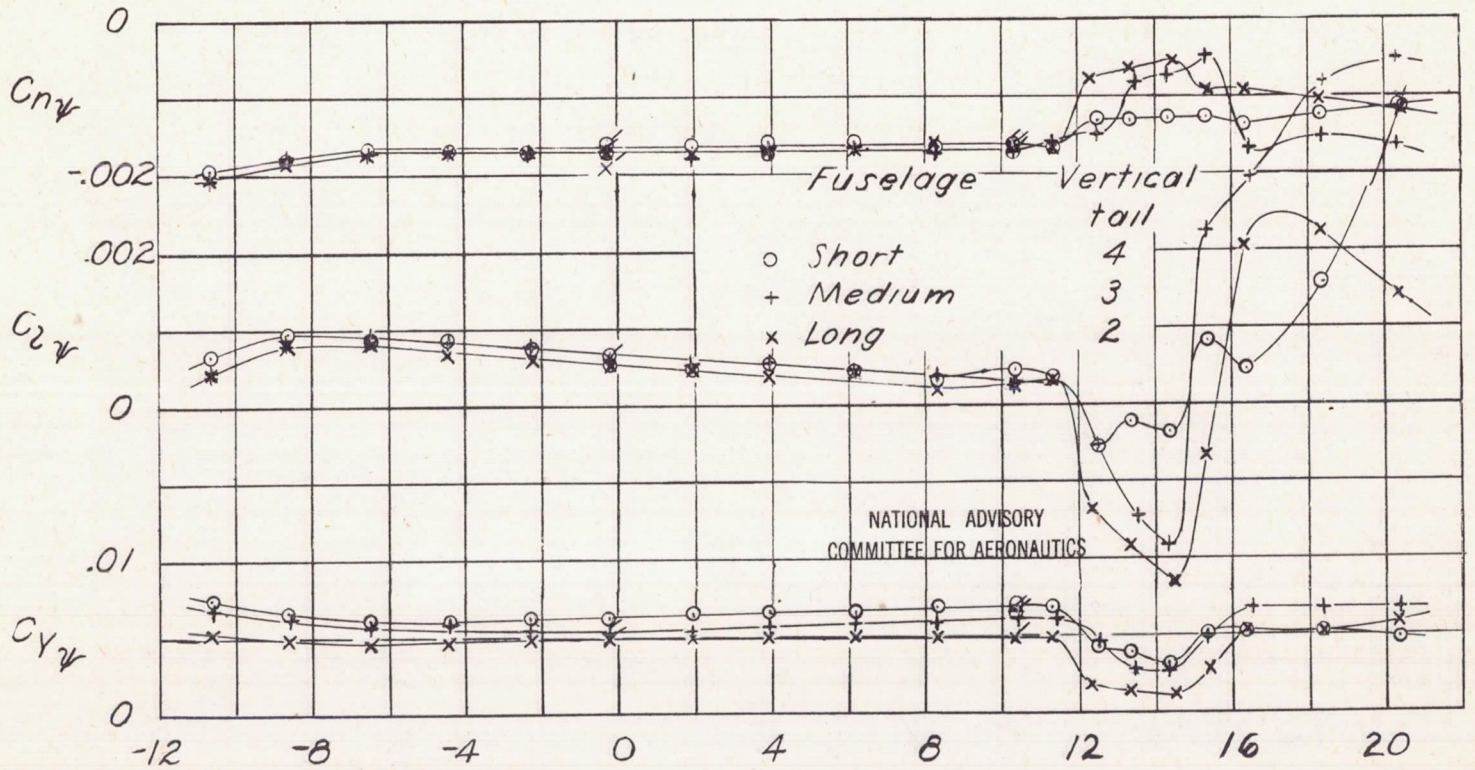

(a) Γ, 0°.

Figure 17.- Effect of several combinations having constant tail volume on variation of lateral-stability slopes C_{n_ψ}, C_{l_ψ}, and C_{Y_ψ} with angle of attack. Tail volume, 0.0407; horizontal tail on; q, 65 lb/sq ft.

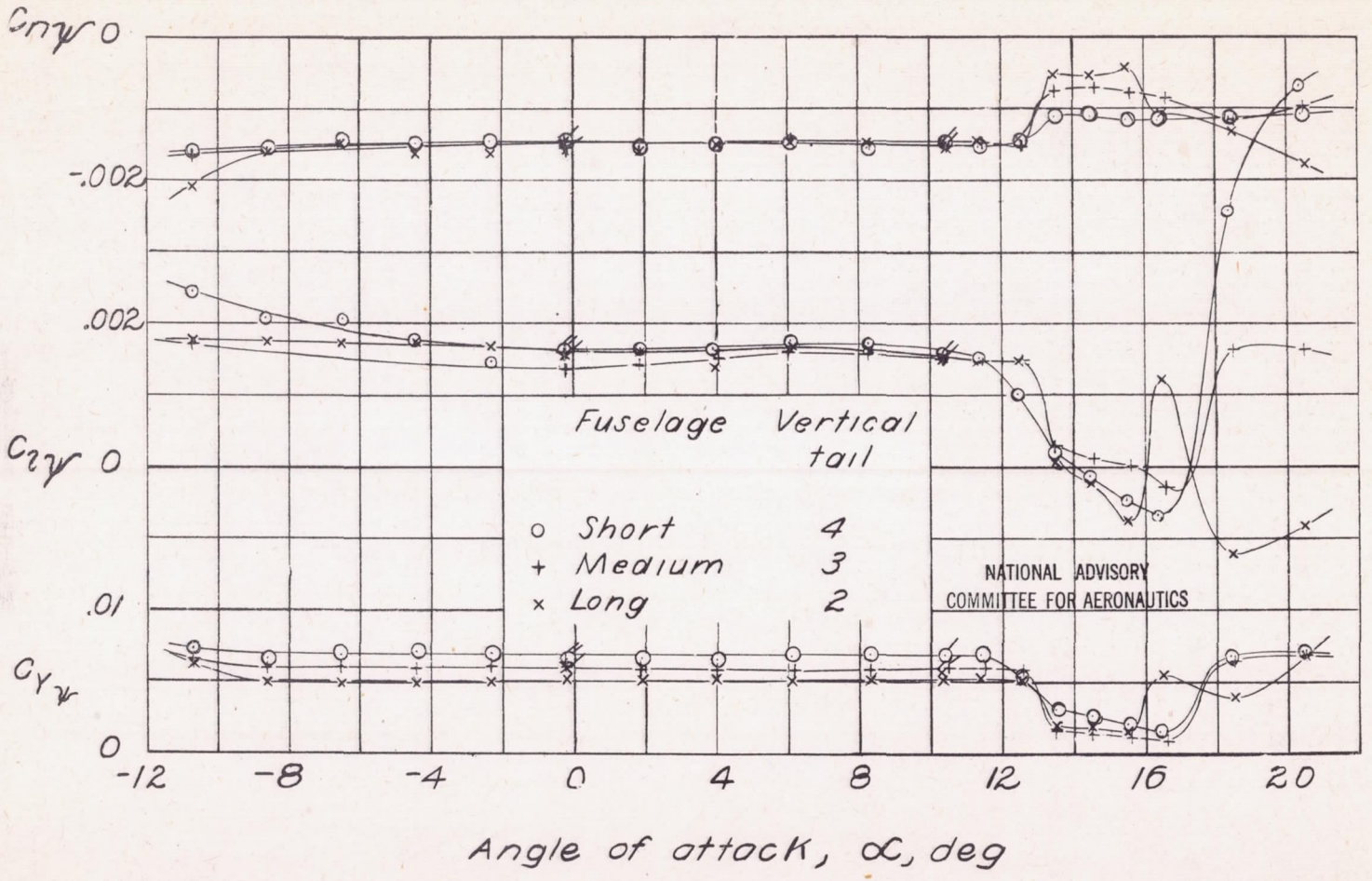

(b) Γ, 5°.

Figure 17.- Concluded.

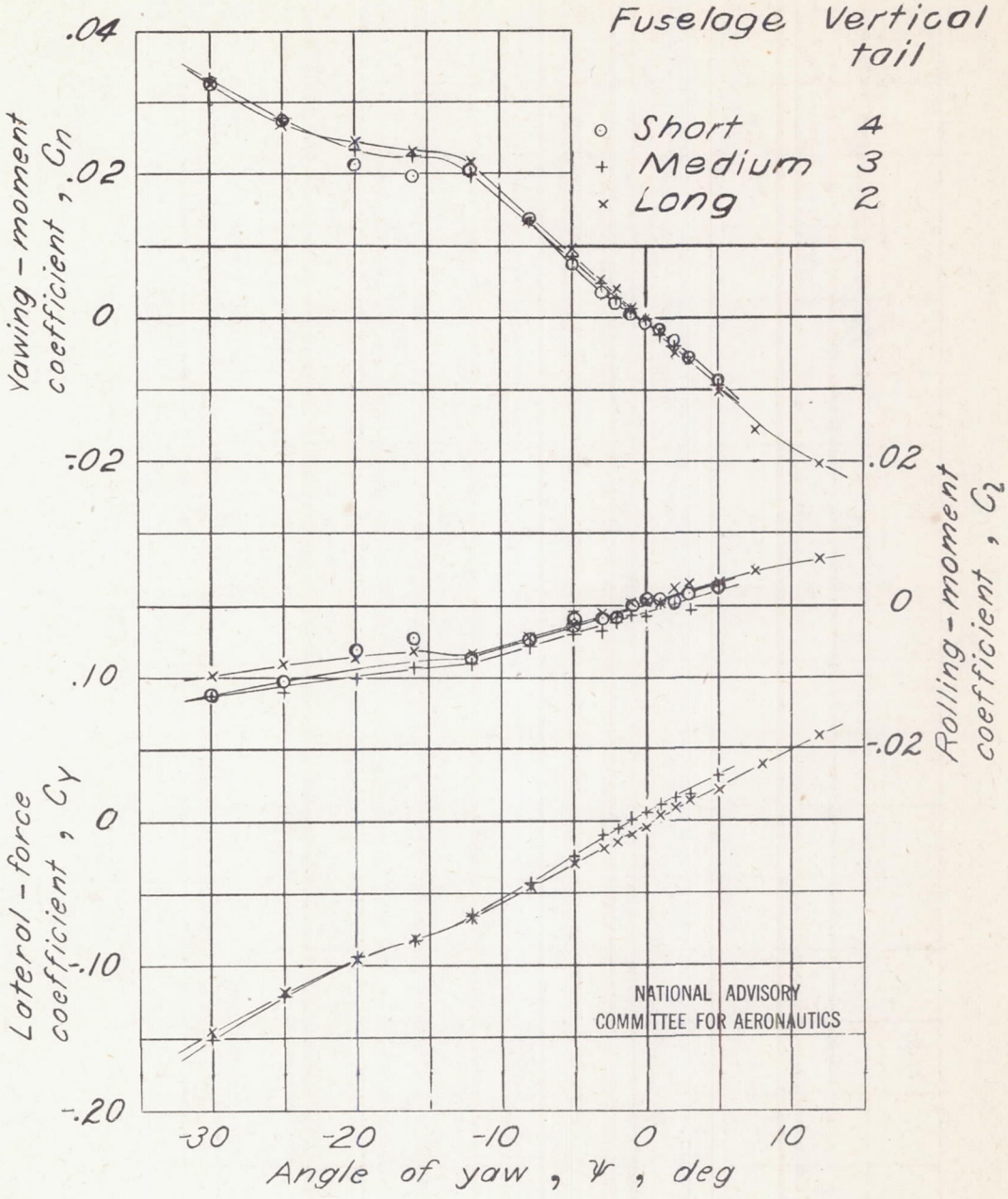

(a) Γ, 0°; α, -0.2°; q, 65 lb/sq ft.

Figure 18.- Effect of several combinations having constant tail volume on variation of yawing-moment, rolling-moment, and lateral-force coefficients with angle of yaw. Tail volume, 0.0407; horizontal tail on.

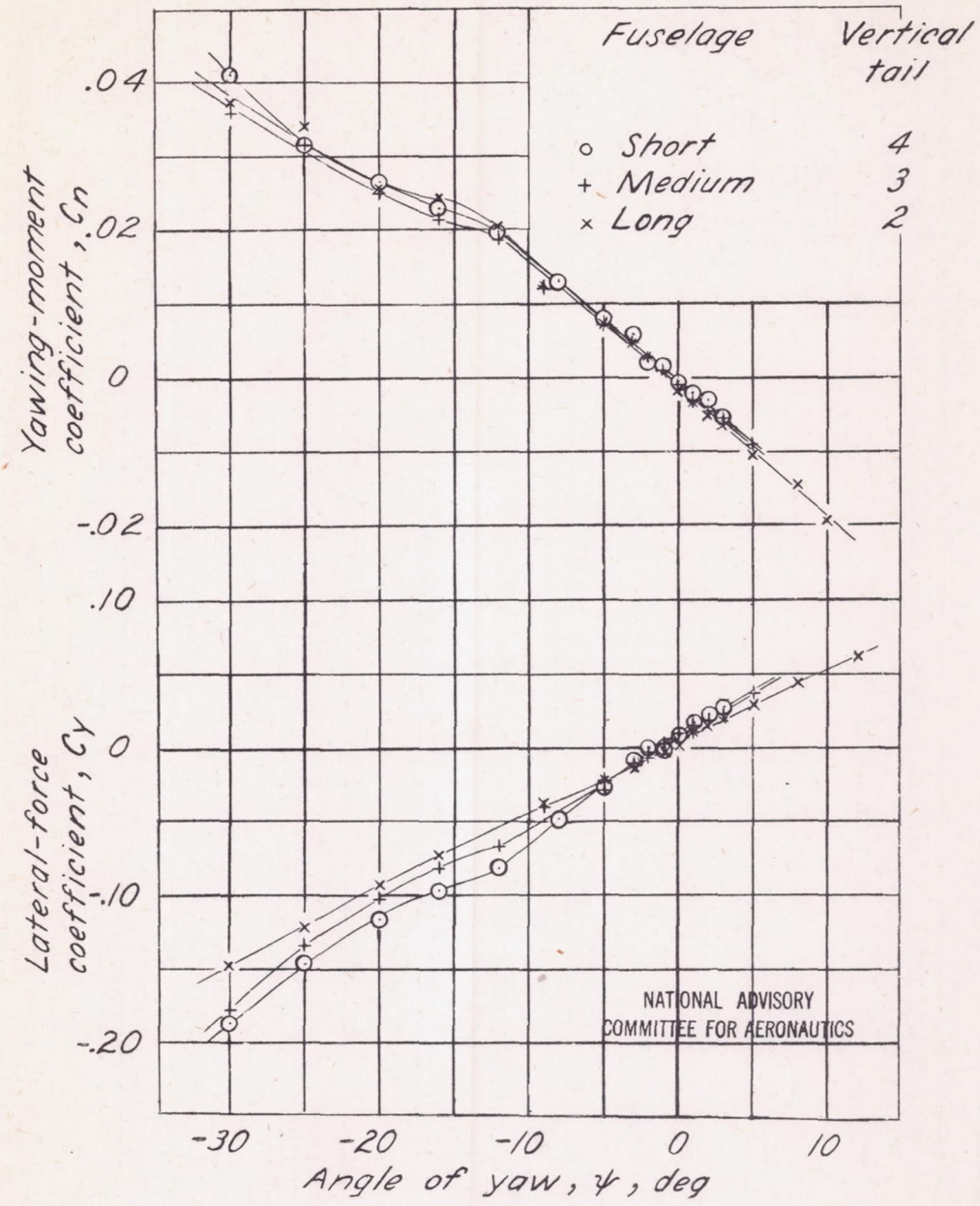

(b) Γ, 0°; α, 10.3°; q, 40 lb/sq ft.

Figure 18.- Continued.

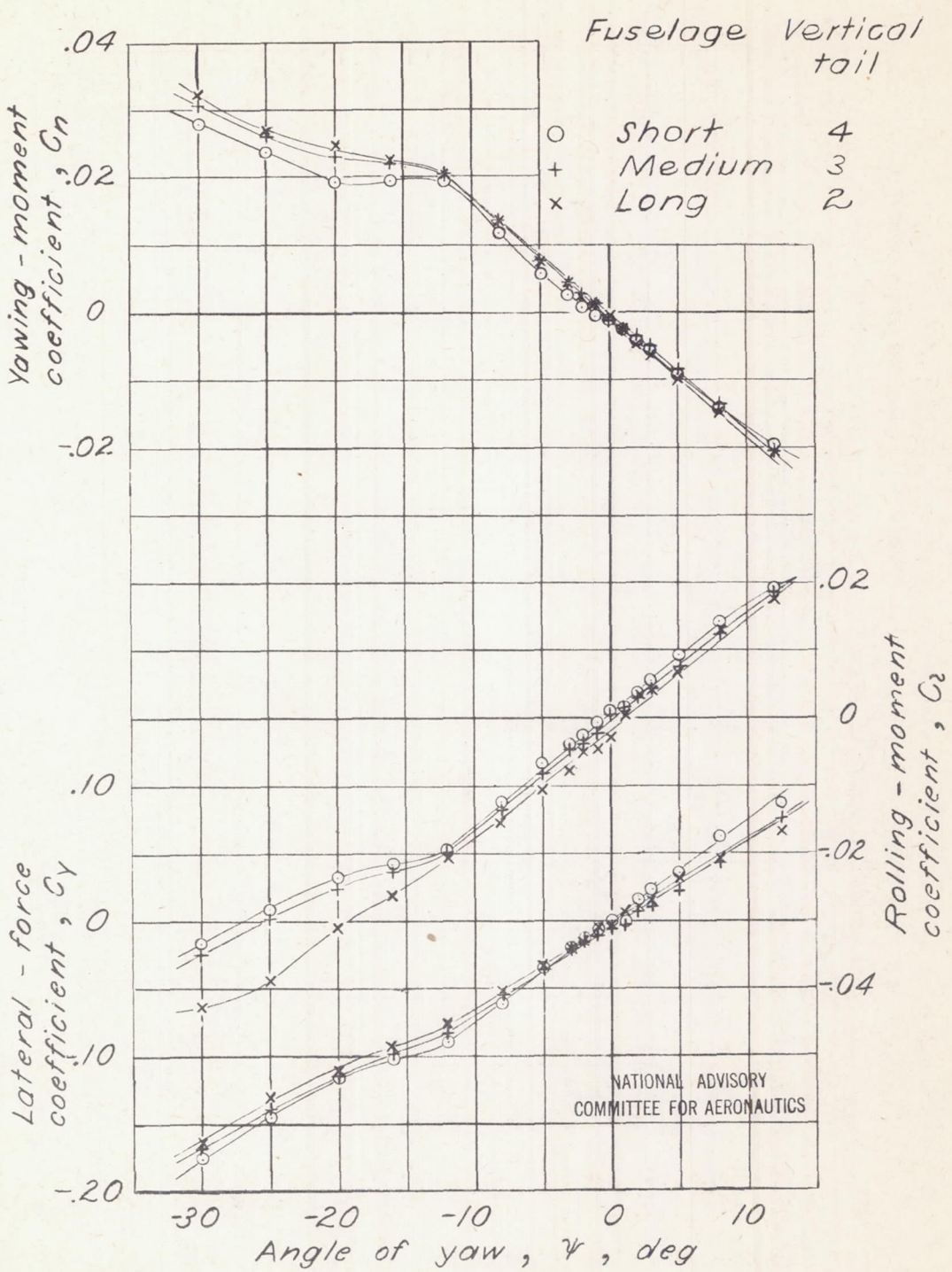

(c) Γ, 5°; α, -0.2°; q, 65 lb/sq ft.

Figure 18.- Continued.

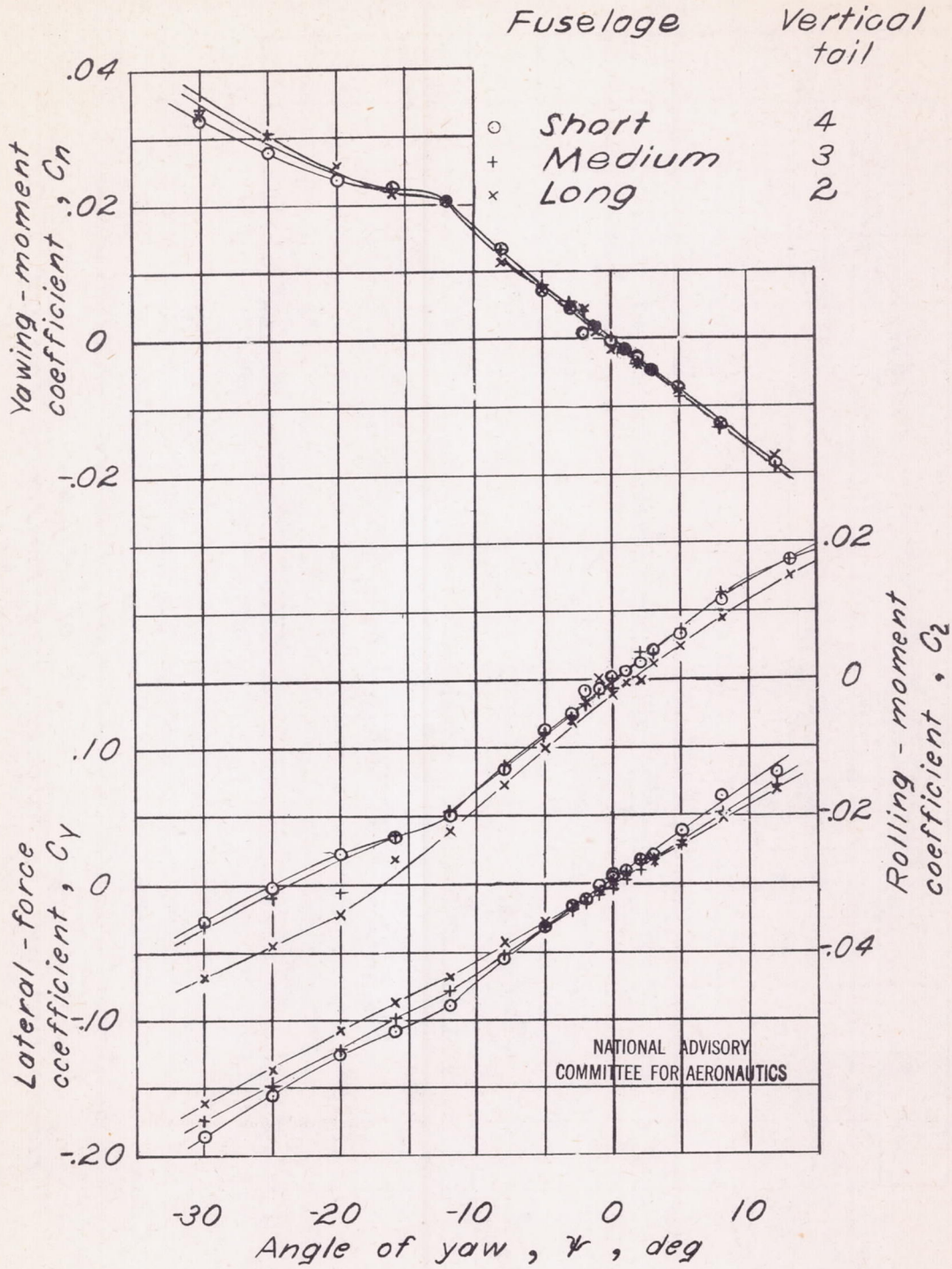

(d) Γ, 5°; α, 10.3°; q, 40 lb/sq ft.

Figure 18.- Concluded.

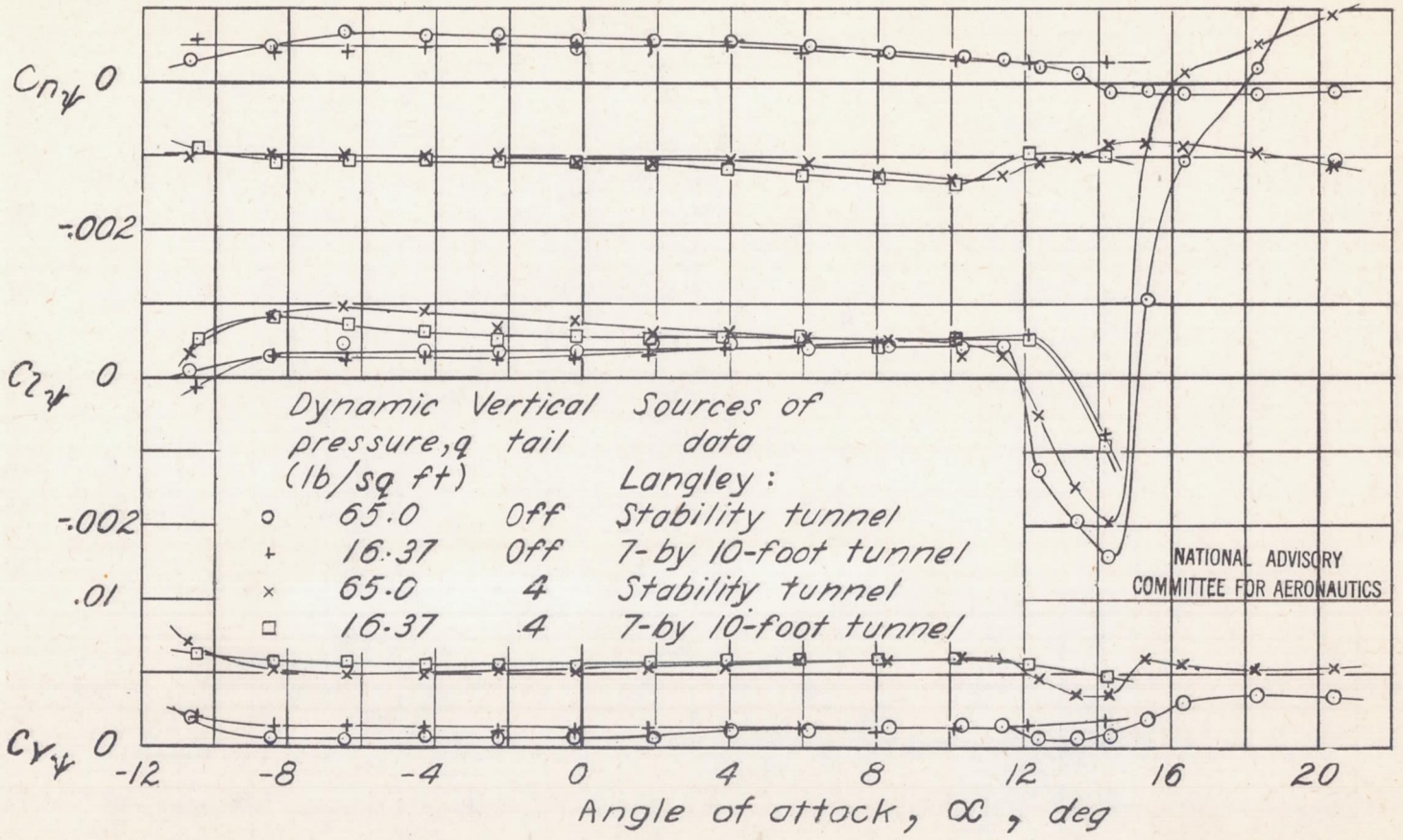

Figure 19. - Comparison of data from Langley stability and Langley 7-by 10-foot tunnels for variation of lateral-stability slopes C_{n_ψ}, C_{l_ψ}, and C_{Y_ψ} with angle of attack. Short fuselage in combination with rectangular wing; horizontal tail off; Γ, 0°.